

2-8
NASA TECHNICAL NOTE

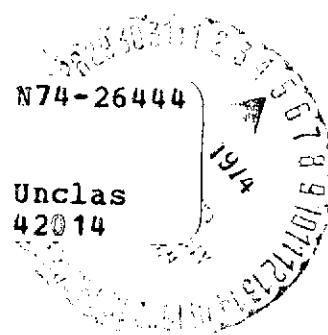


NASA TN D-7583

NASA TN D-7583

(NASA-TN-D-7583) COMPARISONS OF
TWO-DIMENSIONAL SHOCK-EXPANSION THEORY
WITH EXPERIMENTAL AERODYNAMIC DATA FOR
DELTA-PLANFORM WINGS AT HIGH SUPERSONIC
SPEEDS (NASA) 36 p HC \$3.25 CSCL 01B

H1/02



**COMPARISONS OF TWO-DIMENSIONAL
SHOCK-EXPANSION THEORY WITH
EXPERIMENTAL AERODYNAMIC DATA
FOR DELTA-PLANFORM WINGS
AT HIGH SUPERSONIC SPEEDS**

by Lloyd S. Jernell

*Langley Research Center
Hampton, Va. 23665*



NATIONAL AERONAUTICS AND SPACE ADMINISTRATION • WASHINGTON, D. C. • JUNE 1974

1. Report No. NASA TN D-7583		2. Government Accession No.		3. Recipient's Catalog No.	
4. Title and Subtitle COMPARISONS OF TWO-DIMENSIONAL SHOCK-EXPANSION THEORY WITH EXPERIMENTAL AERODYNAMIC DATA FOR DELTA-PLANFORM WINGS AT HIGH SUPERSONIC SPEEDS				5. Report Date June 1974	
				6. Performing Organization Code	
7. Author(s) Lloyd S. Jernell				8. Performing Organization Report No. L-9316	
				10. Work Unit No. 760-66-01-01	
9. Performing Organization Name and Address NASA Langley Research Center Hampton, Va. 23665				11. Contract or Grant No.	
				13. Type of Report and Period Covered Technical Note	
12. Sponsoring Agency Name and Address National Aeronautics and Space Administration Washington, D. C. 20546				14. Sponsoring Agency Code	
15. Supplementary Notes					
16. Abstract An investigation has been conducted to explore the potential for optimizing airfoil shape at high supersonic speeds by utilizing the two-dimensional shock-expansion method. Theoretical and experimental force and moment coefficients are compared for four delta-planform semispan wings having a leading-edge sweep angle of 65° and incorporating modified diamond airfoils with a thickness-chord ratio of 0.06. The wings differ only in airfoil maximum-thickness position and camber. The experimental data are obtained at Mach numbers of 3.95 and 4.63 and at a Reynolds number of 9.84×10^6 per meter. A relatively simple method is developed for predicting, in terms of lift-drag ratio, the optimum modified diamond airfoil at high supersonic and hypersonic speeds.					
17. Key Words (Suggested by Author(s)) Diamond airfoil Delta wing Shock-expansion theory				18. Distribution Statement Unclassified - Unlimited STAR Category 02	
19. Security Classif. (of this report) Unclassified	20. Security Classif. (of this page) Unclassified	21. No. of Pages 36 39	22. Price* \$3.25		

COMPARISONS OF TWO-DIMENSIONAL
SHOCK-EXPANSION THEORY WITH EXPERIMENTAL
AERODYNAMIC DATA FOR DELTA-PLANFORM WINGS
AT HIGH SUPERSONIC SPEEDS

By Lloyd S. Jernell
Langley Research Center

SUMMARY

An investigation has been conducted to explore the potential for optimizing airfoil shape at high supersonic speeds by utilizing the two-dimensional shock-expansion method. Theoretical and experimental force and moment coefficients are compared for four delta-planform semispan wings having a leading-edge sweep angle of 65° and incorporating modified diamond airfoils with a thickness-chord ratio of 0.06. The wings differ only in airfoil maximum-thickness position and camber. The experimental data are obtained at Mach numbers of 3.95 and 4.63 and at a Reynolds number of 9.84×10^6 per meter.

Although maximum lift-drag ratio is overestimated by approximately 6 to 8 percent, theory provides an accurate estimate of the relative effects of airfoil maximum-thickness position and camber. A relatively simple method is developed for predicting, in terms of lift-drag ratio, the optimum modified diamond airfoil at high supersonic and hypersonic speeds.

INTRODUCTION

Two-dimensional shock-expansion theory has been widely used to determine the aerodynamic characteristics of sharp-leading-edge wings. References 1 to 3 present the results of analytical investigations which have employed the shock-expansion method to determine airfoil characteristics at high supersonic and hypersonic speeds. The data of reference 3 indicate that this method provides an accurate estimate of the surface pressure up to arbitrarily high Mach numbers provided the flow acts as an ideal gas and the flow deflection angles are somewhat less than those initiating shock detachment. With regard to a wing of finite span at high Mach numbers, exact numerical solutions to the problem of flow over a flat delta wing with supersonic leading edges are developed for the upper and lower surfaces in references 4 and 5, respectively. In both investigations it is concluded that the normal force is practically independent of sweep angle and may be

approximated by two-dimensional theory. In reference 6 experimental force and pressure data for flat-bottom wings having wedge airfoil sections and sweep angles of 70° and 76° are compared with various theories at a free-stream Mach number of 8.2. Again, the data indicate that the force coefficients may be closely approximated by the two-dimensional shock-expansion theory.

The effectiveness of the shock-expansion method and other theories in predicting the pressure distribution over a wing-body configuration at high supersonic speeds is reported in reference 7. The wing is of delta planform with a sweep angle of 65° and employs a symmetrical diamond airfoil. The data show that at a Mach number of 4.63 and moderate angles of attack (to approximately 11°), the experimental pressure distributions over the wing upper surfaces are practically constant for each flat surface and agree well with the predictions based on two-dimensional Prandtl-Meyer expansion. Although considerable pressure gradient exists over the lower surfaces, the average pressure coefficient for each flat surface differs from the two-dimensional shock-expansion predictions by less than 10 percent. In addition, the data show that as Mach number is increased, there is a decrease in the pressure gradient and an improvement in the agreement between theory and experiment.

The foregoing comparisons suggest the possibility of employing the shock-expansion method to optimize airfoil shape for a finite wing at high supersonic and hypersonic speeds. The primary purpose of this investigation is to explore the potential for such optimization in terms of lift-drag ratio in the high supersonic speed range. The study is limited to a series of modified diamond airfoils in conjunction with delta-planform wings of 65° leading-edge sweep. A relatively simple method is subsequently developed for predicting the optimum modified diamond airfoil, according to the two-dimensional shock-expansion theory, at high supersonic and hypersonic speeds. Theoretical predictions are compared with experimental force and moment coefficients obtained on several semispan wing models which represent a range of airfoil geometry variables spanning the optimum profile. The optimum wing is designed for a free-stream Mach number of 4.63. Experimental data are obtained at Mach numbers of 3.95 and 4.63 and at a Reynolds number of 9.84×10^6 per meter.

SYMBOLS

c	chord
\bar{c}	wing mean geometric chord
C_D	drag coefficient, Drag/qS

C_L	lift coefficient, $Lift/qS$
C_m	pitching-moment coefficient about $\bar{c}/2$, $Pitching\ moment/qS\bar{c}$
C_p	pressure coefficient
D	drag
l	airfoil maximum-thickness position, measured from leading edge
L	lift
L/D	lift-drag ratio, C_L/C_D
$(L/D)_{max}$	maximum lift-drag ratio
M	free-stream Mach number
p	free-stream static pressure
q	free-stream dynamic pressure
S	wing area
t	airfoil thickness
t_{max}	airfoil maximum thickness
t_u	maximum thickness of portion of airfoil above chord line
x	projected length of airfoil surface on horizontal plane (parallel to free-stream flow)
α	angle of attack

Subscripts:

1	airfoil forward lower surface
2	airfoil rearward lower surface

- 3 airfoil forward upper surface
- 4 airfoil rearward upper surface

MODELS AND APPARATUS

Details of the four semispan wings are shown in figure 1. All wings were of delta planform with 65° leading-edge sweep and incorporated modified diamond airfoil sections having a thickness-chord ratio of 0.06. Airfoil geometry variables consisted of camber and longitudinal location of maximum thickness. Wing 1 employed the optimum modified diamond airfoil, based on two-dimensional shock-expansion theory, for a free-stream Mach number of 4.63. The optimization procedure is discussed in the section "Theoretical Considerations." The wings were attached to a four-component strain-gage balance housed within a sting-mounted splitter plate. (See fig. 2.) A gap of approximately 0.07 cm was maintained between the wing and plate to prevent fouling.

Boundary-layer transition strips were placed 1 cm rearward (streamwise) of the wing leading edges. The strips were composed of No. 40 carborundum grains (average diameter approximately 0.046 cm) embedded in a plastic adhesive. The average diameter of the grains was approximately equal to the local boundary-layer thickness at $M = 4.63$ and exceeded the thickness by about 15 percent at $M = 3.95$. Estimates based on the data of reference 8 indicate that the total particle-drag coefficients are within the accuracy of the data.

The investigation was conducted in the high Mach number test section of the Langley Unitary Plan wind tunnel, which is a variable-pressure, continuous-flow facility. The test section is approximately 1.22 meters square by 2.13 meters long. The nozzle leading to the test section is of the asymmetric sliding-block type, which permits a continuous variation in Mach number from about 2.3 to 4.7.

MEASUREMENTS, TEST CONDITIONS, AND ACCURACIES

Aerodynamic forces and moments were measured at Mach numbers of 3.95 and 4.63 and at a Reynolds number of 9.84×10^6 per meter. The angle-of-attack range was approximately -2° to 7° . The dewpoint was maintained below 239 K to minimize moisture condensation effects.

The estimated accuracies, based on instrument calibration and data repeatability, are as follows:

C_D	± 0.0001
C_L	± 0.002
C_m	± 0.0004

THEORETICAL CONSIDERATIONS

In the theoretical procedure employed herein, which utilizes the shock-expansion method, the flow is considered to be two-dimensional and hence affected only by airfoil shape. Figure 3(a) shows the effects of the longitudinal location of maximum thickness $\frac{l}{c}$ on the maximum lift-drag ratio for various degrees of camber $\frac{t_u}{t_{\max}}$ as predicted by the two-dimensional shock-expansion method for a series of modified diamond airfoils having a thickness-chord ratio of 0.06. The data are computed for inviscid flow and a free-stream Mach number of 4.63. It should be noted that the peak values of maximum lift-drag ratio occur at $\frac{l}{c} \approx 0.60$. A cross plot of these data, presented in figure 3(b), exhibits a peak value at $\frac{t_u}{t_{\max}} \approx 0.60$. Thus, the optimum modified diamond airfoil, in terms of maximum lift-drag ratio, has the maximum thickness located at approximately the 60-percent-chord station and is cambered so that approximately 60 percent of the thickness is above the chord line.

It was noticed during these calculations that for the more efficient airfoils, the pressure coefficients on the forward upper surface $C_{p,3}$ and the rearward lower surface $C_{p,2}$ were very small at the inviscid $\left(\frac{L}{D}\right)_{\max}$; for the optimum airfoil $\left(\frac{l}{c} = 0.60, \frac{t_u}{t_{\max}} = 0.60\right)$, for all practical purposes, these pressure coefficients could be considered zero. This trend is demonstrated in figure 4, which shows the corresponding variation of pressure coefficient and lift-drag ratio with angle of attack for the optimum profile (design M of 4.63, $\frac{t_{\max}}{c} = 0.06$). It is seen that at the maximum lift-drag ratio $C_{p,3}$ and $C_{p,2}$ are essentially zero. This relationship indicates that at the optimum angle of attack, surface 3 is approximately parallel to the free-stream flow and, for the relatively thin airfoils considered, that surface 2 is also approximately parallel to the free stream. This relationship allows the use of a relatively simple optimization procedure instead of the laborious method employed to obtain the data of figure 3. In figure 5, surfaces 2 and 3 are placed parallel to the free-stream flow. By assuming a wing-section width of unity, the following equation can be obtained:

$$\begin{aligned}
C_L &= \frac{L}{qS} \\
&= \frac{1}{qc} \left[(p_1 - p)x_1 + (p_2 - p)x_2 - (p_3 - p)x_3 - (p_4 - p)x_4 \right] \\
&= \frac{p_1 - p}{q} \frac{x_1}{c} + \frac{p_2 - p}{q} \frac{x_2}{c} - \frac{p_3 - p}{q} \frac{x_3}{c} - \frac{p_4 - p}{q} \frac{x_4}{c} \\
&= C_{p,1} \frac{x_1}{c} + C_{p,2} \frac{x_2}{c} - C_{p,3} \frac{x_3}{c} - C_{p,4} \frac{x_4}{c}
\end{aligned}$$

Since $C_{p,3} = 0$ and, for the relatively thin airfoils considered, $C_{p,2} \approx 0$

$$\begin{aligned}
C_L &= C_{p,1} \frac{x_1}{c} - C_{p,4} \frac{x_4}{c} \\
&= \frac{C_{p,1}}{c} (c \cos \alpha - x_2) - \frac{C_{p,4}}{c} (c \cos \alpha - x_3) \\
&= \frac{C_{p,1}}{c} \left(c \cos \alpha - \frac{c - l}{\cos \alpha} \right) - \frac{C_{p,4}}{c} \left(c \cos \alpha - \frac{l}{\cos \alpha} \right)
\end{aligned}$$

Thus

$$C_L = C_{p,1} \left(\cos \alpha - \frac{1 - \frac{l}{c}}{\cos \alpha} \right) - C_{p,4} \left(\cos \alpha - \frac{\frac{l}{c}}{\cos \alpha} \right) \quad (1)$$

Similarly,

$$\begin{aligned}
C_D &= \frac{D}{qS} \\
&= \frac{1}{qc} \left[(p_1 - p) t_{\max} \cos \alpha - (p_4 - p) t_{\max} \cos \alpha \right] \\
&= \frac{p_1 - p}{q} \frac{t_{\max}}{c} \cos \alpha - \frac{p_4 - p}{q} \frac{t_{\max}}{c} \cos \alpha
\end{aligned}$$

and

$$C_D = (C_{p,1} - C_{p,4}) \frac{t_{\max}}{c} \cos \alpha \quad (2)$$

Since $\cos \alpha$ is very nearly unity, equations (1) and (2), respectively, reduce to

$$C_L = C_{p,1} \frac{l}{c} - C_{p,4} \left(1 - \frac{l}{c}\right) \quad (3)$$

$$C_D = (C_{p,1} - C_{p,4}) \frac{t_{\max}}{c} \quad (4)$$

Hence

$$\frac{L}{D} = \frac{C_{p,1} \frac{l}{c} - C_{p,4} \left(1 - \frac{l}{c}\right)}{(C_{p,1} - C_{p,4}) \frac{t_{\max}}{c}} \quad (5)$$

It should be pointed out that since surfaces 2 and 3 are assumed to be parallel to the free-stream flow, $\frac{l}{c}$ and $\frac{t_u}{t_{\max}}$ are always equal. A plot of this relationship is shown in figure 6 for $\frac{t_{\max}}{c} = 0.06$ and free-stream Mach numbers of 4.63, 6.00, and 8.00. It should be noted that for $M = 4.63$, the peak value of lift-drag ratio occurs at $\frac{l}{c} \approx 0.60$, which defines an airfoil of geometry essentially the same as the optimum shape obtained by the iterative procedure initially employed. For the higher Mach numbers the data of figure 6 indicate that the airfoil shapes are optimized at $\frac{l}{c}$ approximately equal to 0.63 and 0.69 for Mach numbers of 6.00 and 8.00, respectively. Also of interest is the appreciable increase in the optimum lift-drag ratio with increasing Mach number.

Figure 7 shows the variation of $\left(\frac{L}{D}\right)_{\max}$ with $\frac{l}{c}$ for Mach numbers of 6.00 and 8.00, based on the shock-expansion method, for the optimum $\frac{t_u}{t_{\max}}$ values predicted by equation (5) $\left(\frac{t_u}{t_{\max}} \text{ is equal to } \frac{l}{c} \text{ if surfaces 2 and 3 are assumed to be parallel (see fig. 5)}\right)$. Calculations for $M = 4.63$ are included for comparison. The symbols represent the optimum configurations according to equation (5). Similar data are presented in figure 8 for the variation of $\left(\frac{L}{D}\right)_{\max}$ with $\frac{t_u}{t_{\max}}$, based on the shock-expansion method, for the optimum $\frac{l}{c}$ values as predicted by equation (5). Although analytical data were calculated for limited ranges of maximum-thickness location and camber at Mach numbers of 6.00 and 8.00, the data of figures 7 and 8 indicate that equation (5) also provides close agreement with the shock-expansion method in predicting the optimum modified diamond airfoil at these higher Mach numbers.

COMPARISON OF THEORY AND EXPERIMENT

Comparisons of the two-dimensional shock-expansion predictions with experimental data at Mach numbers of 3.95 and 4.63 are presented in figures 9 to 12 for wings 1 to 4, respectively. It should be emphasized that the theoretical method considers the flow to be two dimensional and hence affected only by airfoil shape. In all cases the predicted pitching-moment coefficients are in excellent agreement with the experimental values. Theory underestimates lift coefficient, with the difference increasing with angle of attack. At angles near cruise attitude ($3^\circ \lesssim \alpha \lesssim 5^\circ$) the decrement ranges from 3 to 7 percent.

The predicted drag coefficients are considerably less than the experimental values, with the decrement in minimum drag coefficient ranging from about 12 to 17 percent at $M = 4.63$ and from about 15 to 19 percent at $M = 3.95$. The theoretical values include viscous effects based on the T' method of reference 9 and the assumption that fully developed turbulent flow exists over that portion of the wing rearward of the boundary-layer transition strips. The results of the evaluations reported in references 10 and 11 indicate that the theoretical skin-friction coefficients predicted by the T' method of reference 9 agree well with experimental data in the Mach number range considered herein. It is believed that the underestimation of drag coefficient is due primarily to the unaccounted-for contribution of the three-dimensional effects of wave drag.

A summary of the theoretical and experimental maximum lift-drag ratio is presented in figure 13. Theory provides an accurate estimate of the relative effects of maximum-thickness position and camber on maximum lift-drag ratio; however, maximum lift-drag ratio is overestimated by approximately 6 to 8 percent. Although the amount of experimental data is limited, the results of figure 13 suggest that for the Mach numbers of this investigation and $\frac{t_u}{t_{\max}} = 0.60$, the optimum location of maximum thickness is in the 60- to 65-percent-chord range and agrees closely with the theoretical predictions. Insufficient test data are available to indicate the optimum camber, but the values obtained exhibit trends paralleling those of theory. Hence, although additional data might be desired to define the optimum airfoil geometry more clearly, the data obtained show that the two-dimensional shock-expansion method is very useful in estimating the optimum airfoil shape for a finite wing at high supersonic and hypersonic speeds.

CONCLUSIONS

An investigation has been conducted to explore the potential for optimizing airfoil shape at high supersonic speeds by utilizing the two-dimensional shock-expansion method. Theoretical data are compared with the experimental force and moment coefficients obtained on four delta-planform semispan wings having a leading-edge sweep angle of 65° and incorporating modified diamond airfoils with a thickness-chord ratio of 0.06. The

wings differ only in airfoil maximum-thickness position and camber. The experimental data are obtained at Mach numbers of 3.95 and 4.63 and at a Reynolds number of 9.84×10^6 per meter. The conclusions are as follows:

1. A relatively simple method is developed for predicting, in terms of lift-drag ratio, the optimum modified diamond airfoil at high supersonic and hypersonic speeds.

2. Although maximum lift-drag ratio is overestimated by approximately 6 to 8 percent, theory provides an accurate estimate of the relative effects of airfoil maximum-thickness position and camber.

3. Theory underestimates lift coefficient, with the difference increasing with angle of attack. At angles of attack near cruise attitude ($3^\circ \lesssim \alpha \lesssim 5^\circ$) the decrement ranges from 3 to 7 percent.

4. The predicted drag coefficients are considerably less than the experimental values, with the decrement in minimum drag coefficient ranging from about 12 to 17 percent at a Mach number of 4.63 and from about 15 to 19 percent at a Mach number of 3.95.

5. The predicted pitching-moment coefficients are in excellent agreement with the experimental values.

Langley Research Center,
National Aeronautics and Space Administration,
Hampton, Va., April 3, 1974.

REFERENCES

1. Linnell, Richard D. : Two-Dimensional Airfoils in Hypersonic Flows. J. Aeronaut. Sci., vol. 16, no. 1, Jan. 1949, pp. 22-30.
2. Dorrance, William H. : Two-Dimensional Airfoils at Moderate Hypersonic Velocities. J. Aeronaut. Sci., vol. 19, no. 9, Sept. 1952, pp. 593-600.
3. Eggers, A. J., Jr.; Syvertson, Clarence A.; and Kraus, Samuel: A Study of Inviscid Flow About Airfoils at High Supersonic Speeds. NACA Rep. 1123, 1953. (Supercedes NACA TN 2646 by Eggers and Syvertson and NACA TN 2729 by Kraus.)
4. Babayev, D. A. : Numerical Solution of the Problem of Flow Round the Upper Surface of a Triangular Wing by a Supersonic Stream. U.S.S.R. Comput. Math. & Math. Phys., no. 2, 1963, pp. 296-308.
5. Babaev, D. A. : Numerical Solution of the Problem of Supersonic Flow Past the Lower Surface of a Delta Wing. AIAA J., vol. 1, no. 9, Sept. 1963, pp. 2224-2231.
6. Rao, D. M. : An Experimental Study of the Hypersonic Aerodynamics of Delta Wings. J. Aeronaut. Soc. India, vol. 23, no. 4, Nov. 1971, pp. 183-190.
7. Jernell, Lloyd S. : Comparisons of Theoretical and Experimental Pressure Distributions Over a Wing-Body Model at High Supersonic Speeds. NASA TN D-6480, 1971.
8. Stallings, Robert L., Jr.; Lamb, Milton; and Howell, Dorothy T. : Drag Characteristics of Circular Cylinders in a Laminar Boundary Layer at Supersonic Free-Stream Velocities. NASA TN D-7369, 1973.
9. Sommer, Simon C.; and Short, Barbara J. : Free-Flight Measurements of Turbulent-Boundary-Layer Skin Friction in the Presence of Severe Aerodynamic Heating at Mach Numbers From 2.8 to 7.0. NACA TN 3391, 1955.
10. Peterson, John B., Jr. : A Comparison of Experimental and Theoretical Results for the Compressible Turbulent-Boundary-Layer Skin Friction With Zero Pressure Gradient. NASA TN D-1795, 1963.
11. Hopkins, Edward J.; and Inouye, Mamoru: An Evaluation of Theories for Predicting Turbulent Skin Friction and Heat Transfer on Flat Plates at Supersonic and Hypersonic Mach Numbers. AIAA J., vol. 9, no. 6, June 1971, pp. 993-1003.

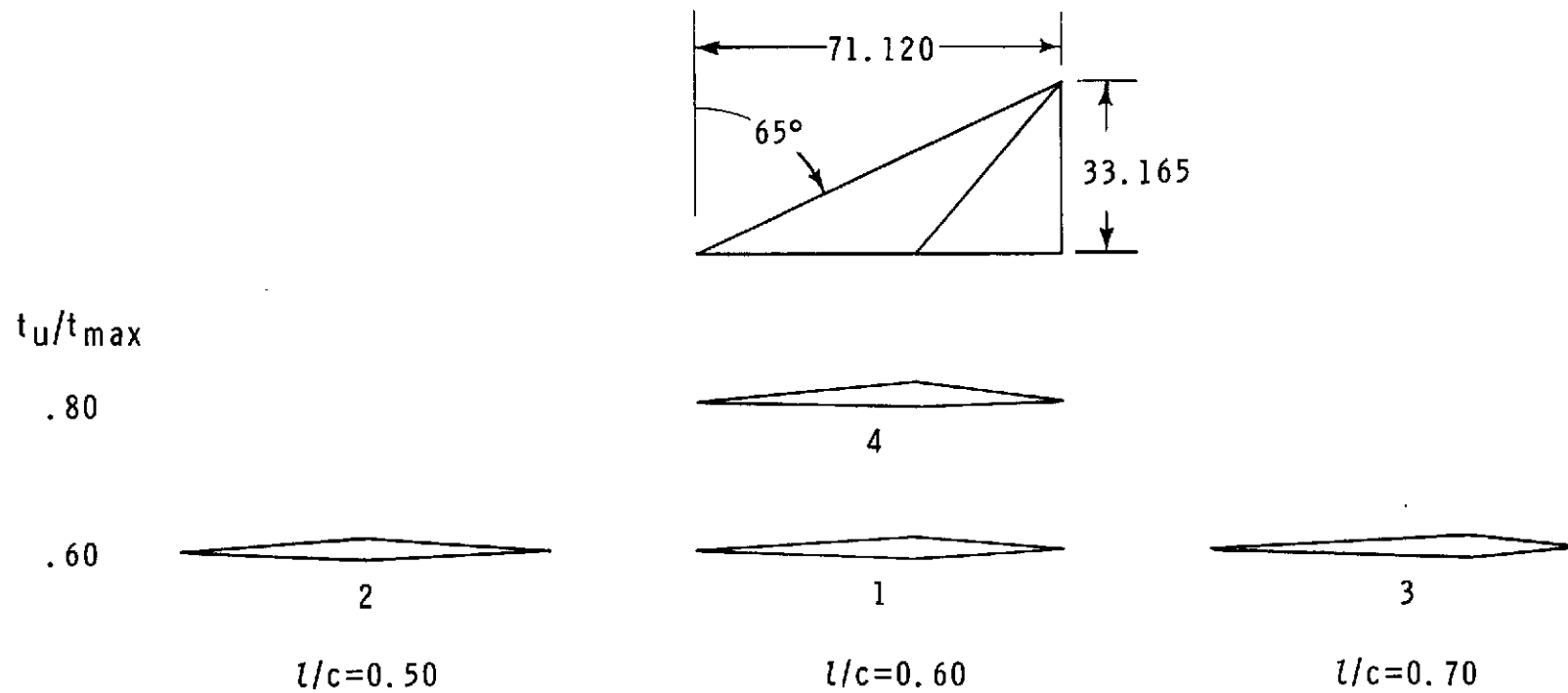


Figure 1.- Model details. Linear dimensions are in centimeters.

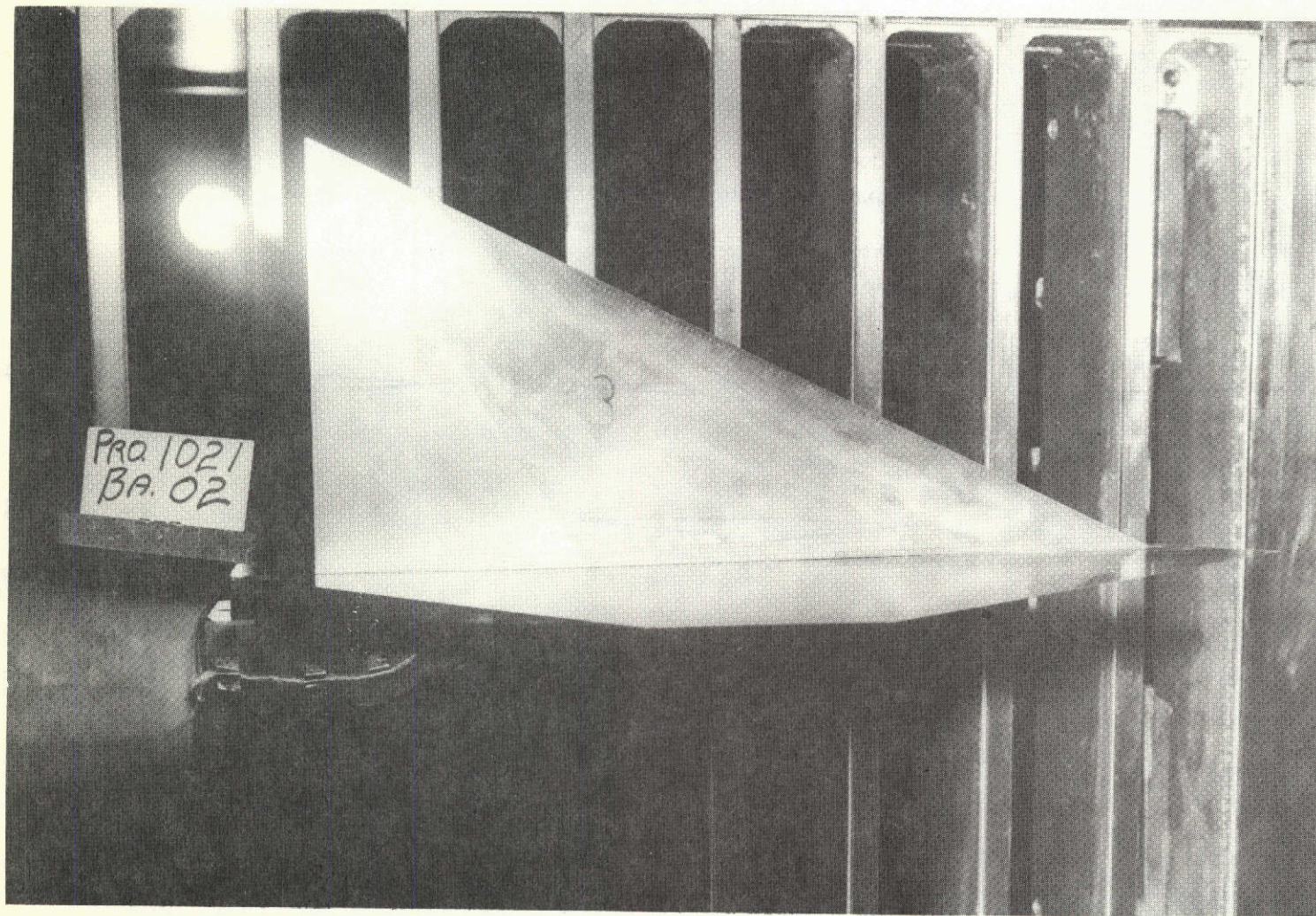
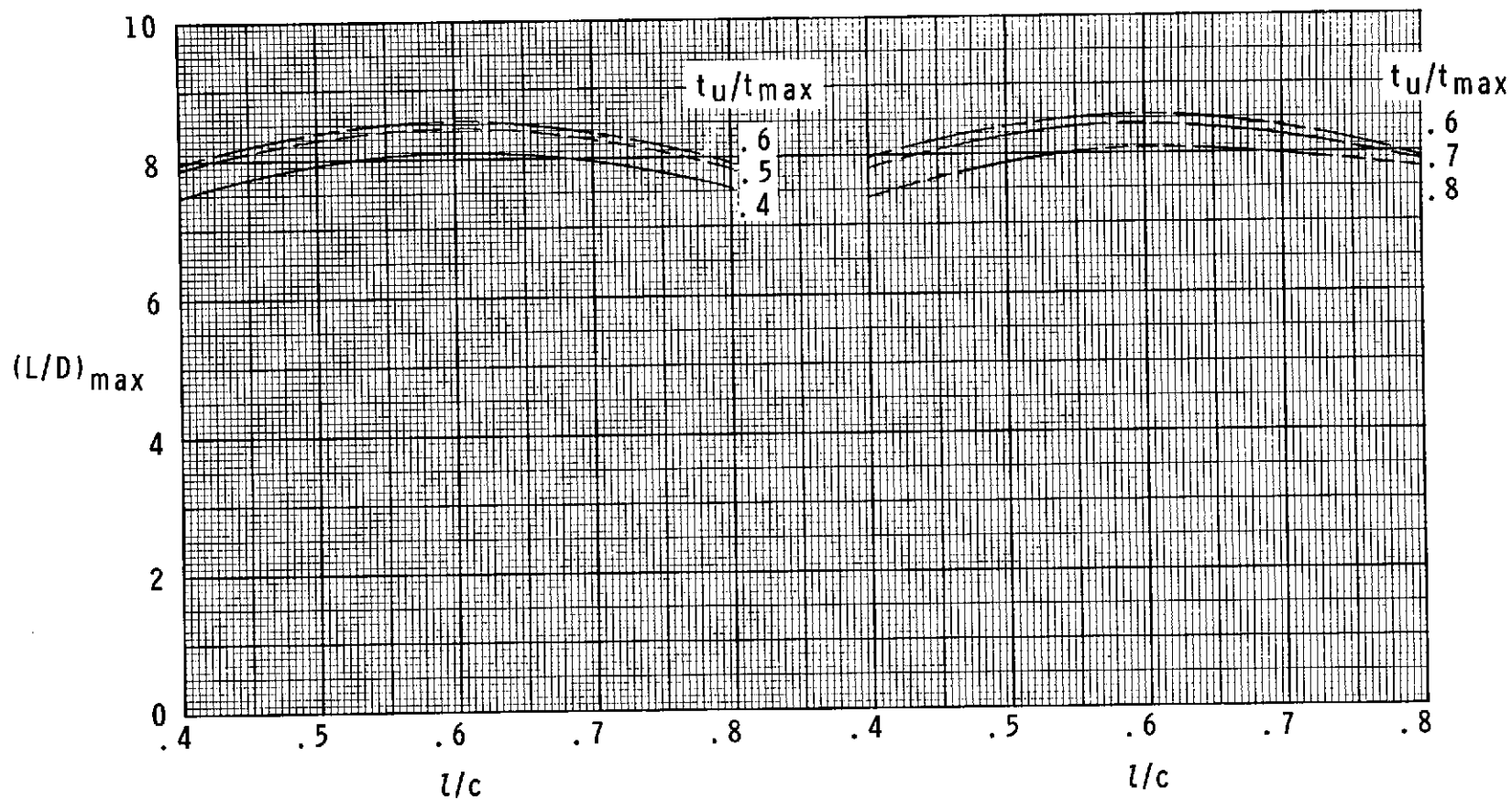


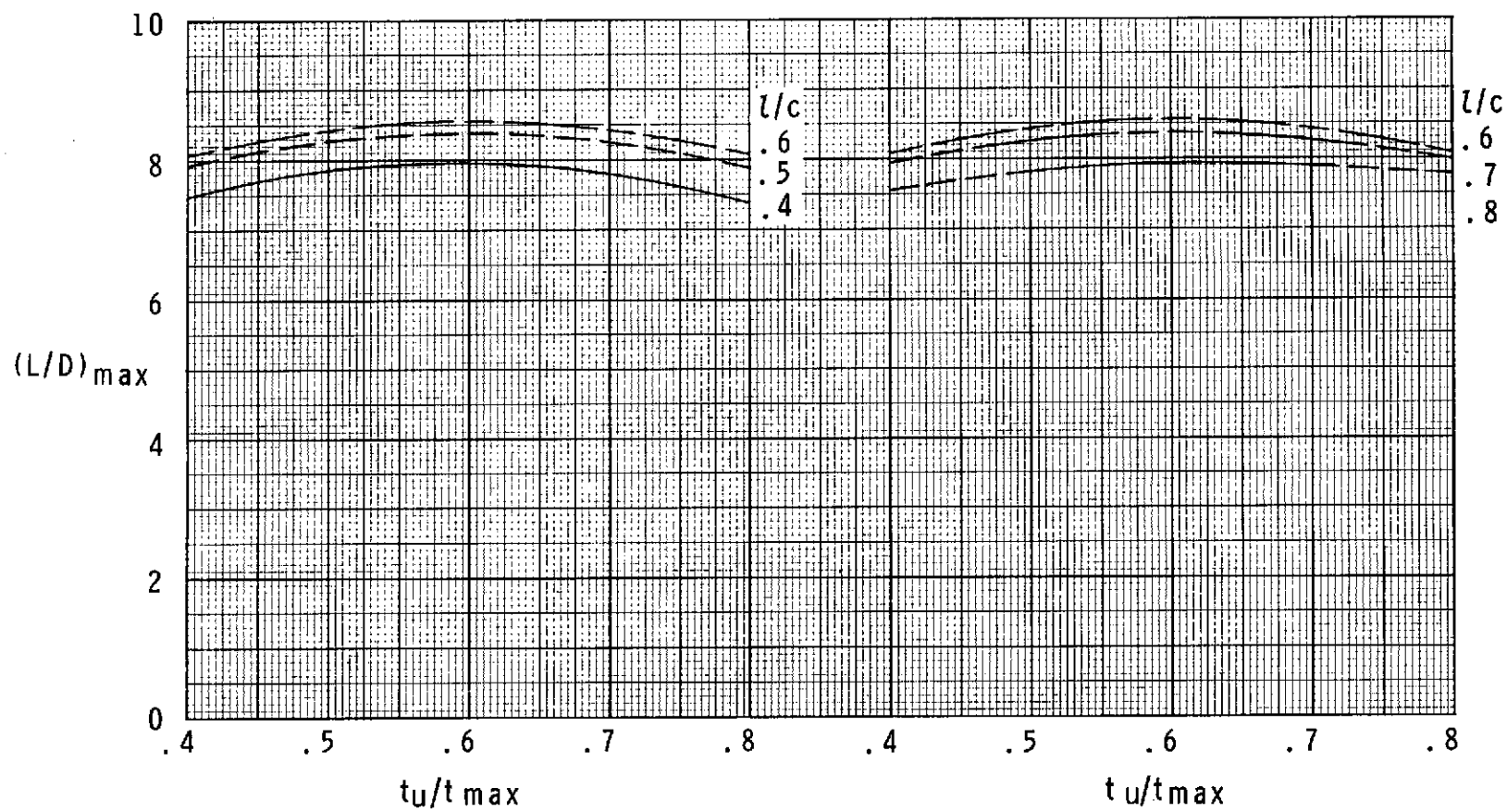
Figure 2.- Tunnel installation.

L-73-3266



(a) Effects of l/c at constant t_u/t_{\max} .

Figure 3.- Maximum lift-drag ratio as predicted by two-dimensional shock-expansion method. Inviscid flow;
 $M = 4.63$; $t/c = 0.06$.



(b) Effects of t_u/t_{\max} at constant l/c .

Figure 3.- Concluded.

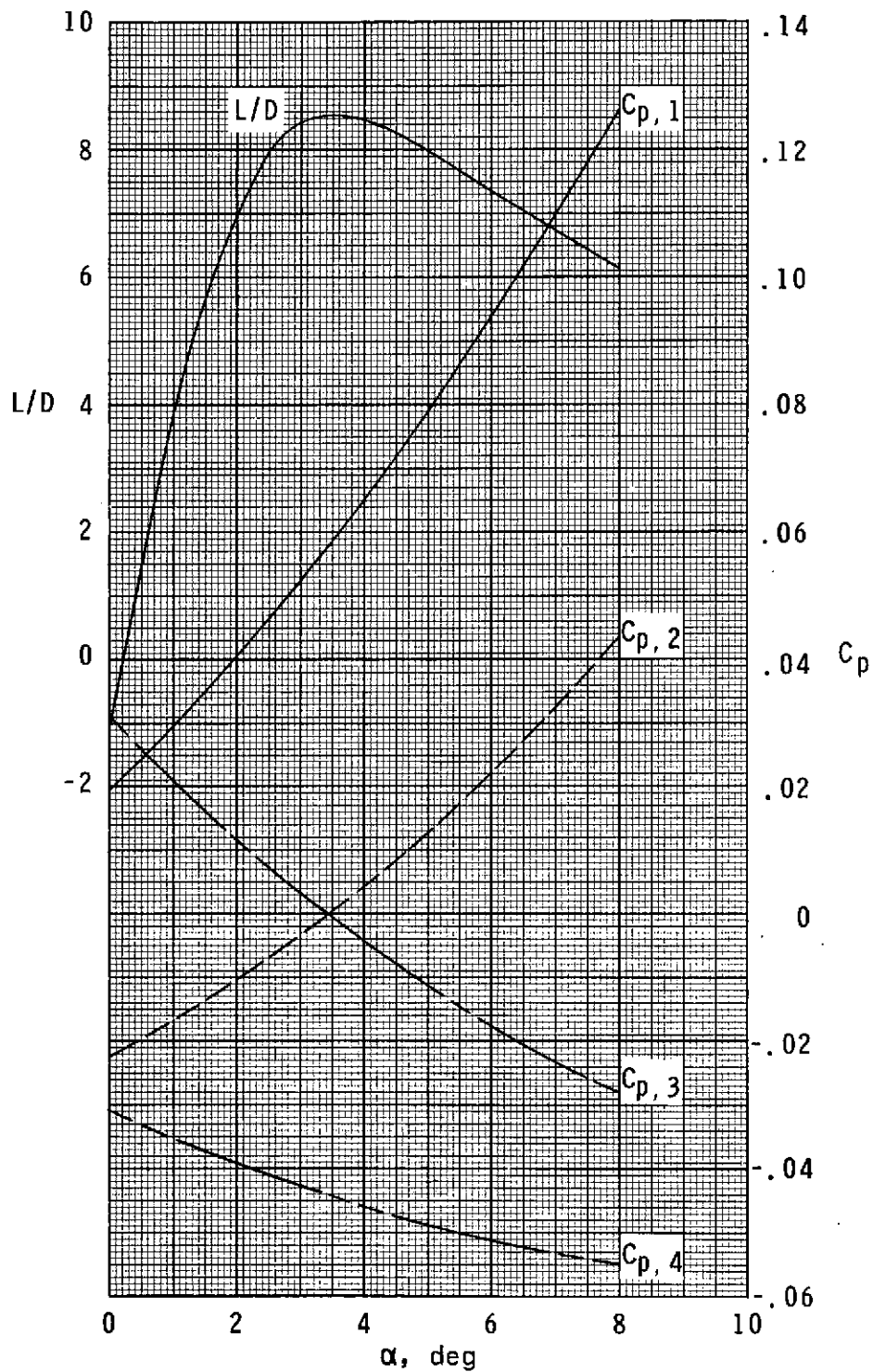


Figure 4.- Variation of pressure coefficient and lift-drag ratio with angle of attack for optimum profile. Design Mach number of 4.63; inviscid flow; $\frac{t_{\max}}{c} = 0.06$.

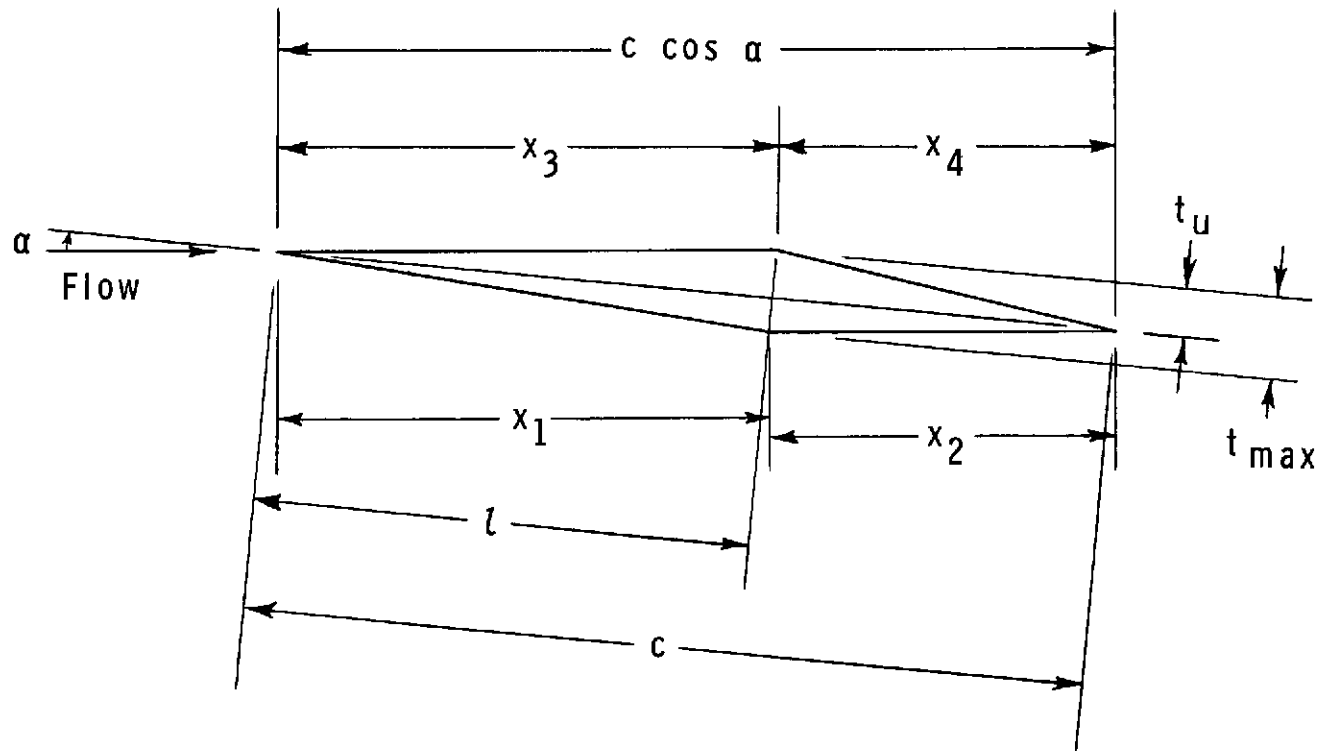


Figure 5.- Sketch of flow problem.

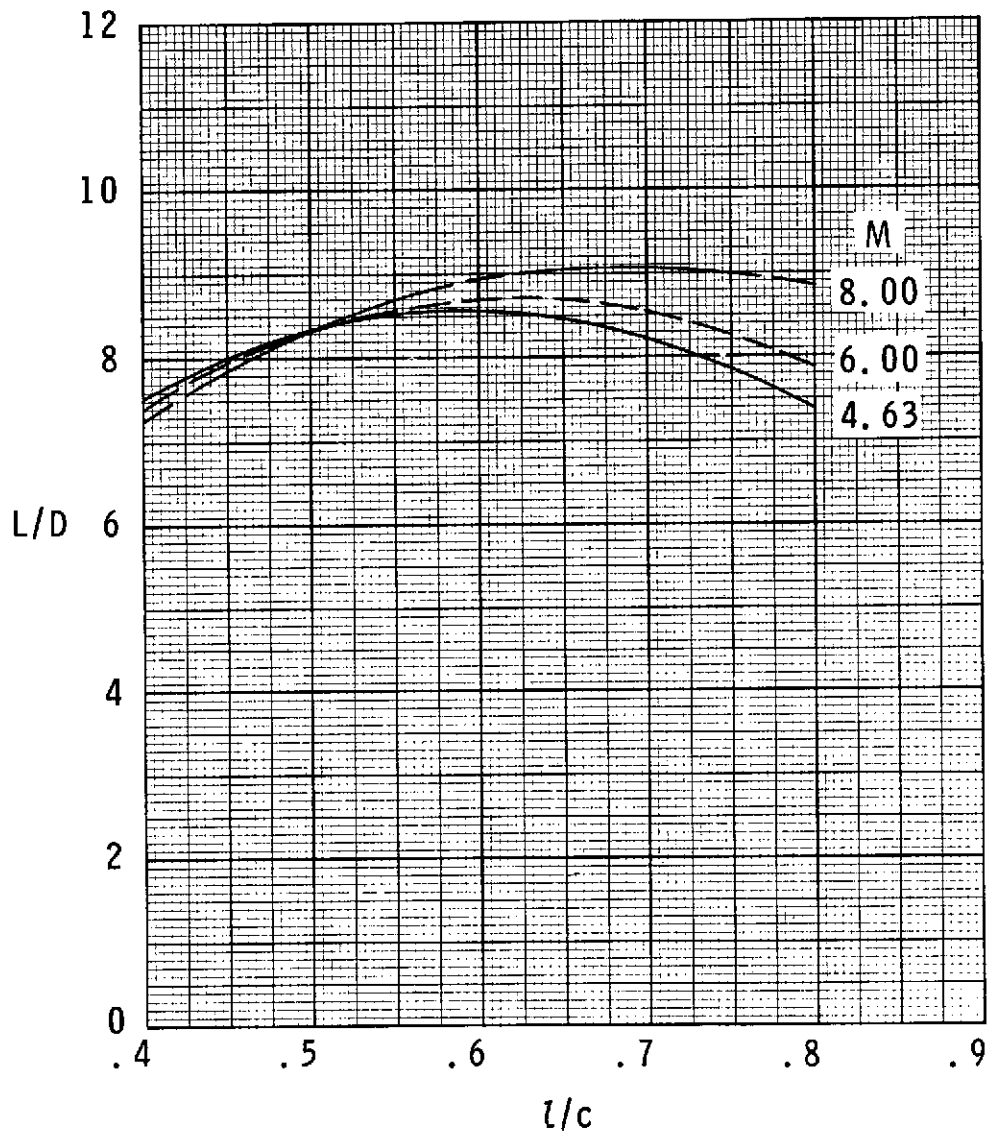


Figure 6.- Variation of L/D with l/c , based on equation (5).
Inviscid flow; $\frac{t_{\max}}{c} = 0.06$.

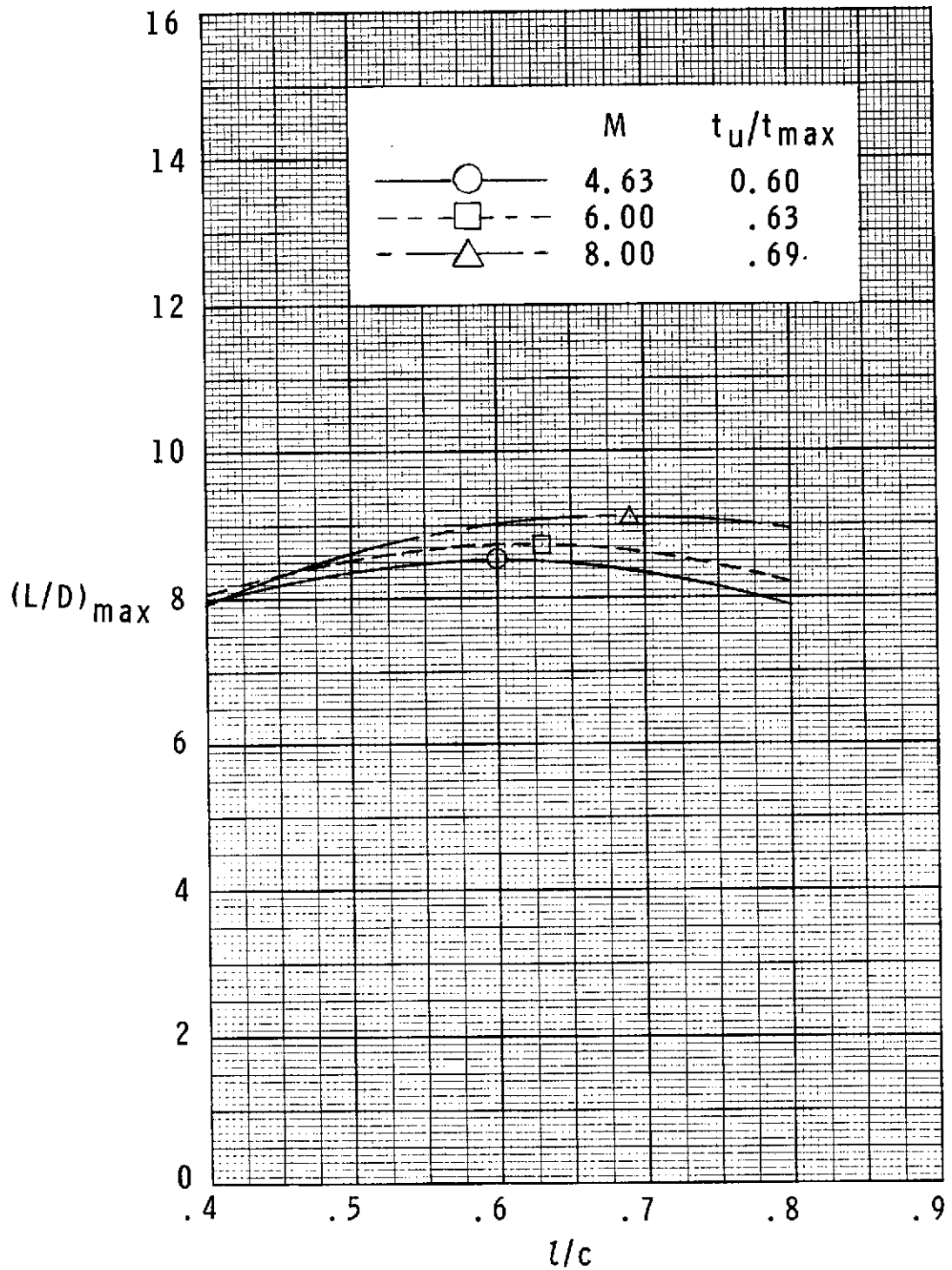


Figure 7.- Variation of $(L/D)_{\max}$ with l/c , based on shock-expansion method, for optimum t_u/t_{\max} values predicted by equation (5). Symbols represent optimum airfoils according to equation (5).

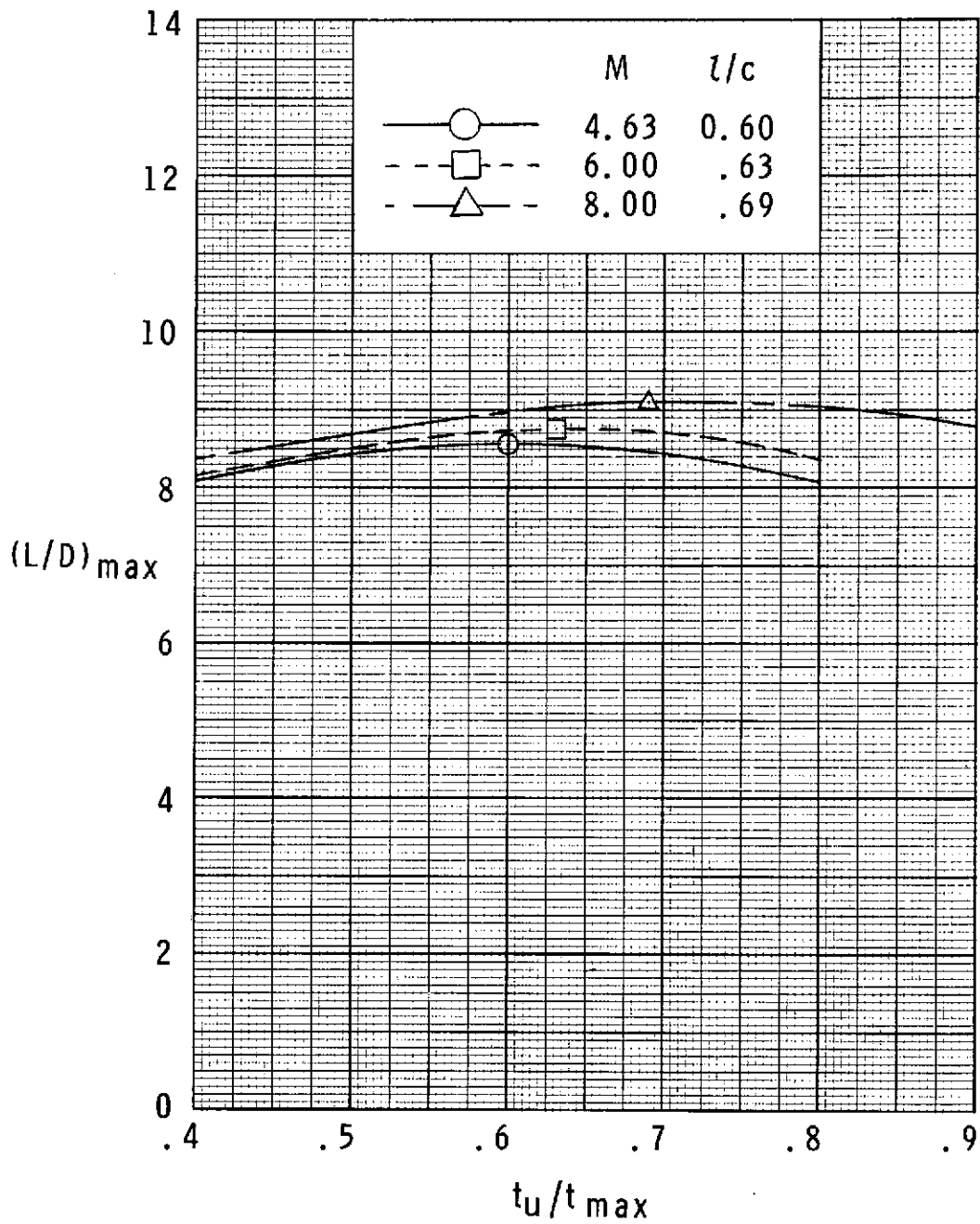
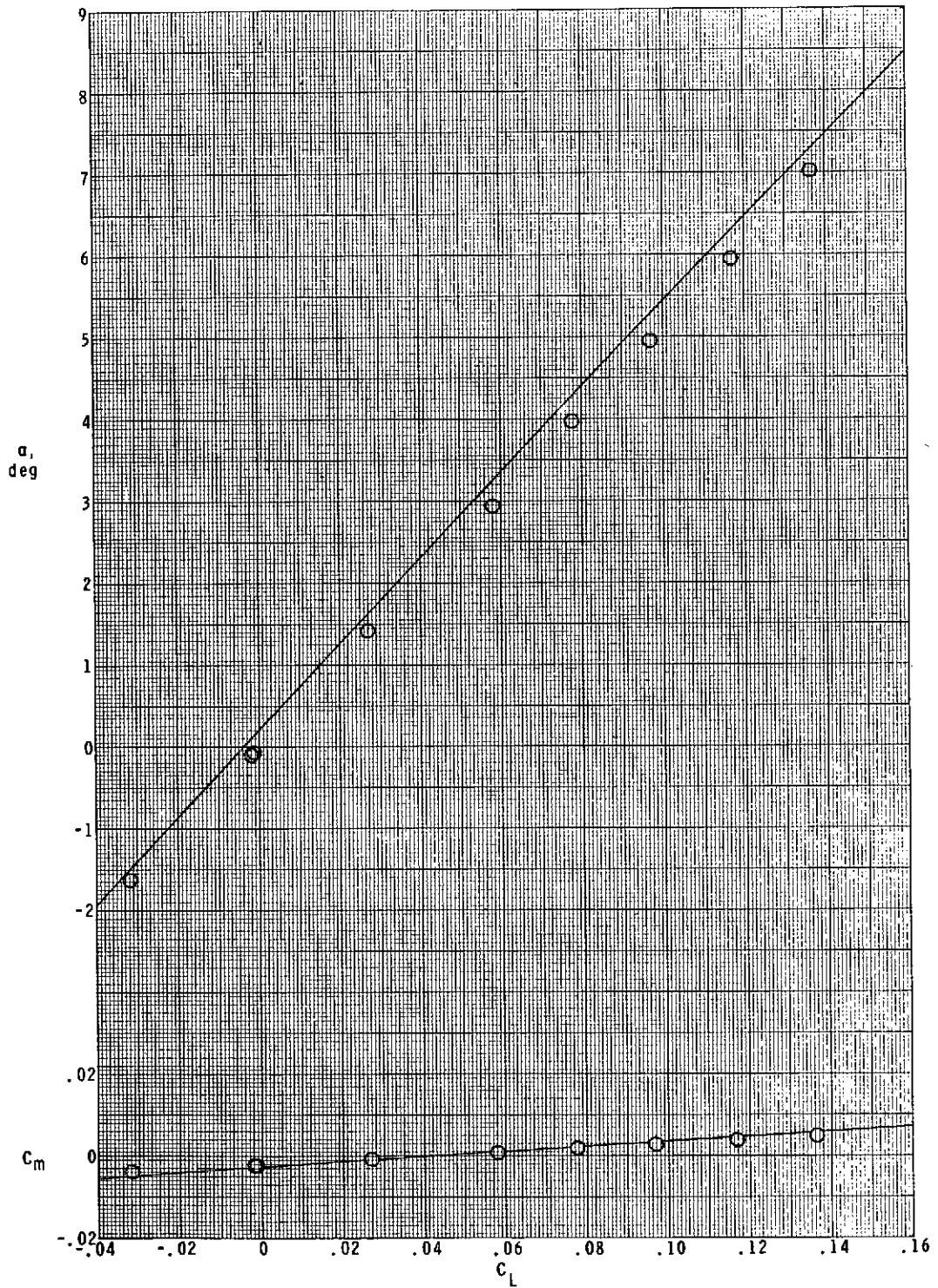
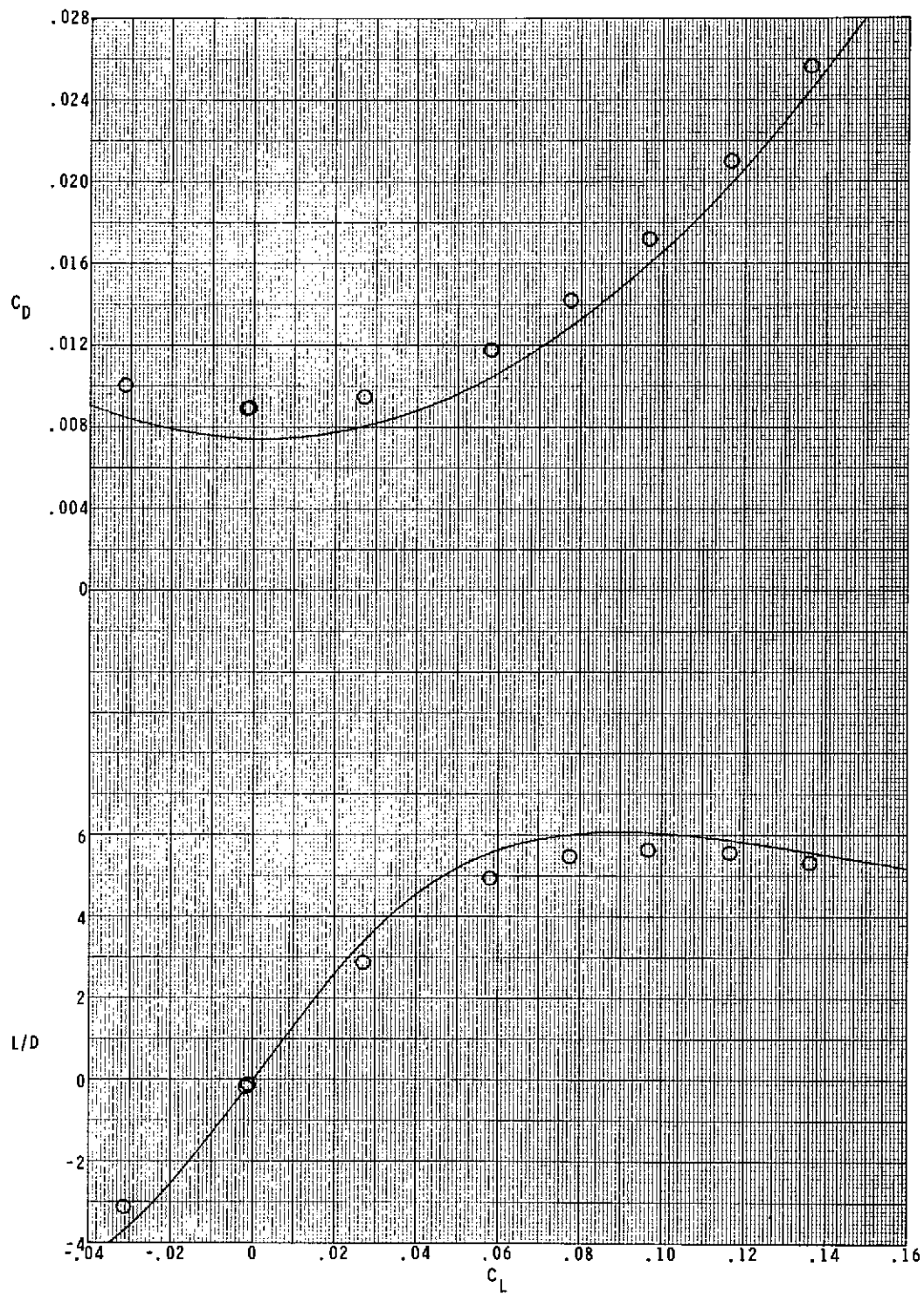


Figure 8.- Variation of $(L/D)_{max}$ with t_u/t_{max} , based on shock-expansion method, for optimum l/c values predicted by equation (5). Symbols represent optimum airfoils according to equation (5).



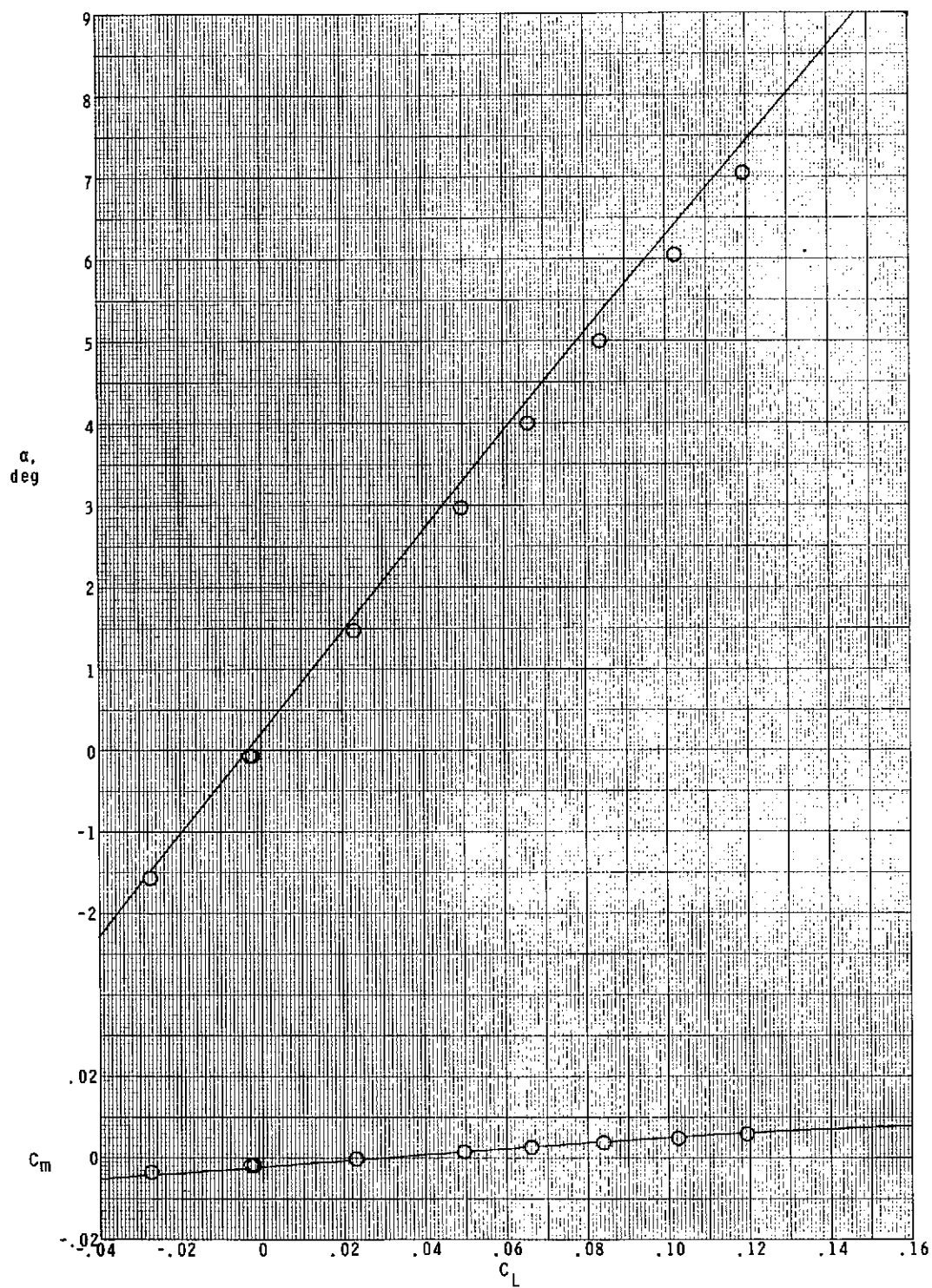
(a) $M = 3.95$.

Figure 9.- Comparison of wing 1 experimental data with two-dimensional shock-expansion predictions. Theory (solid line) includes viscous effects.



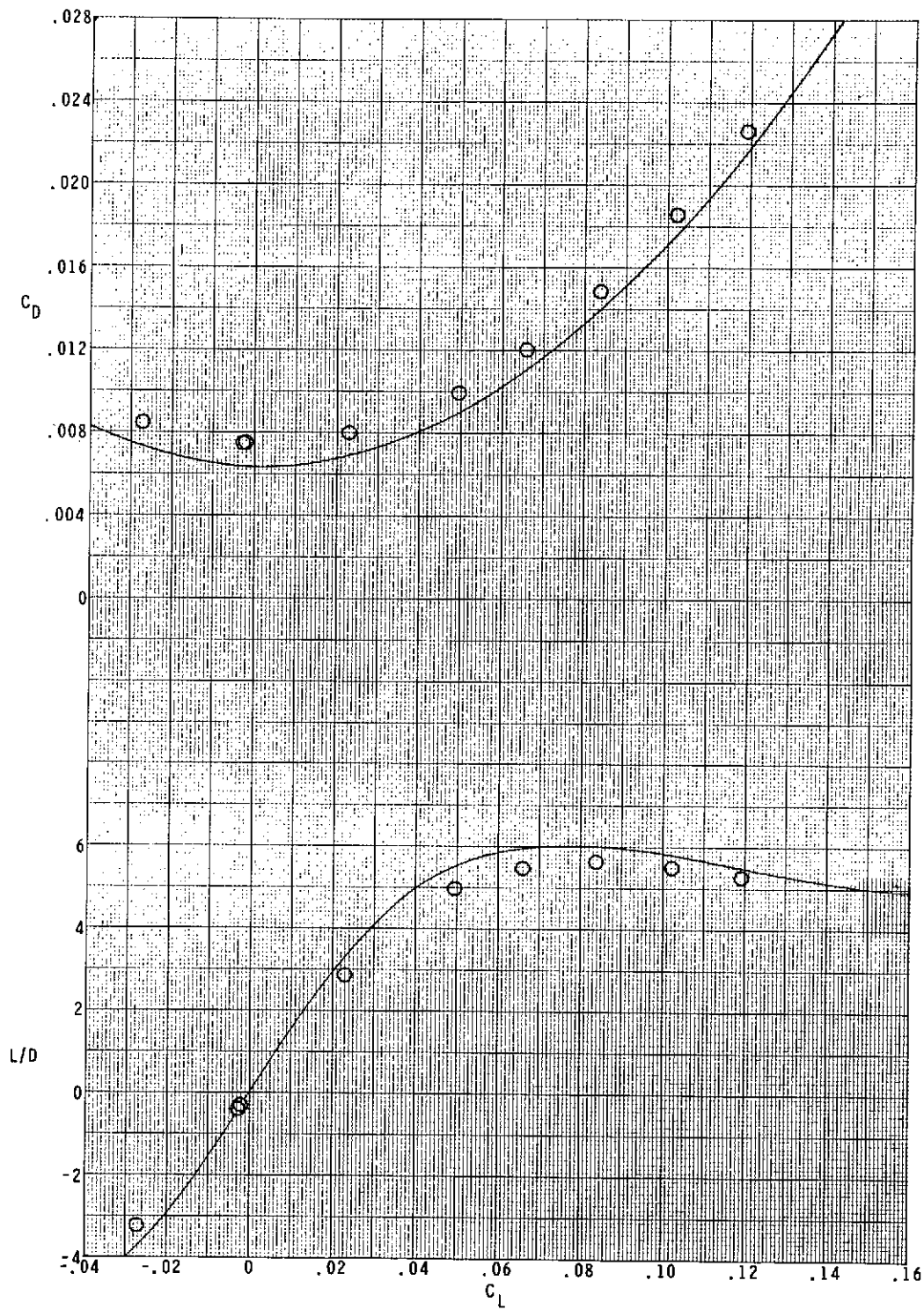
(a) $M = 3.95$. Concluded.

Figure 9.- Continued.



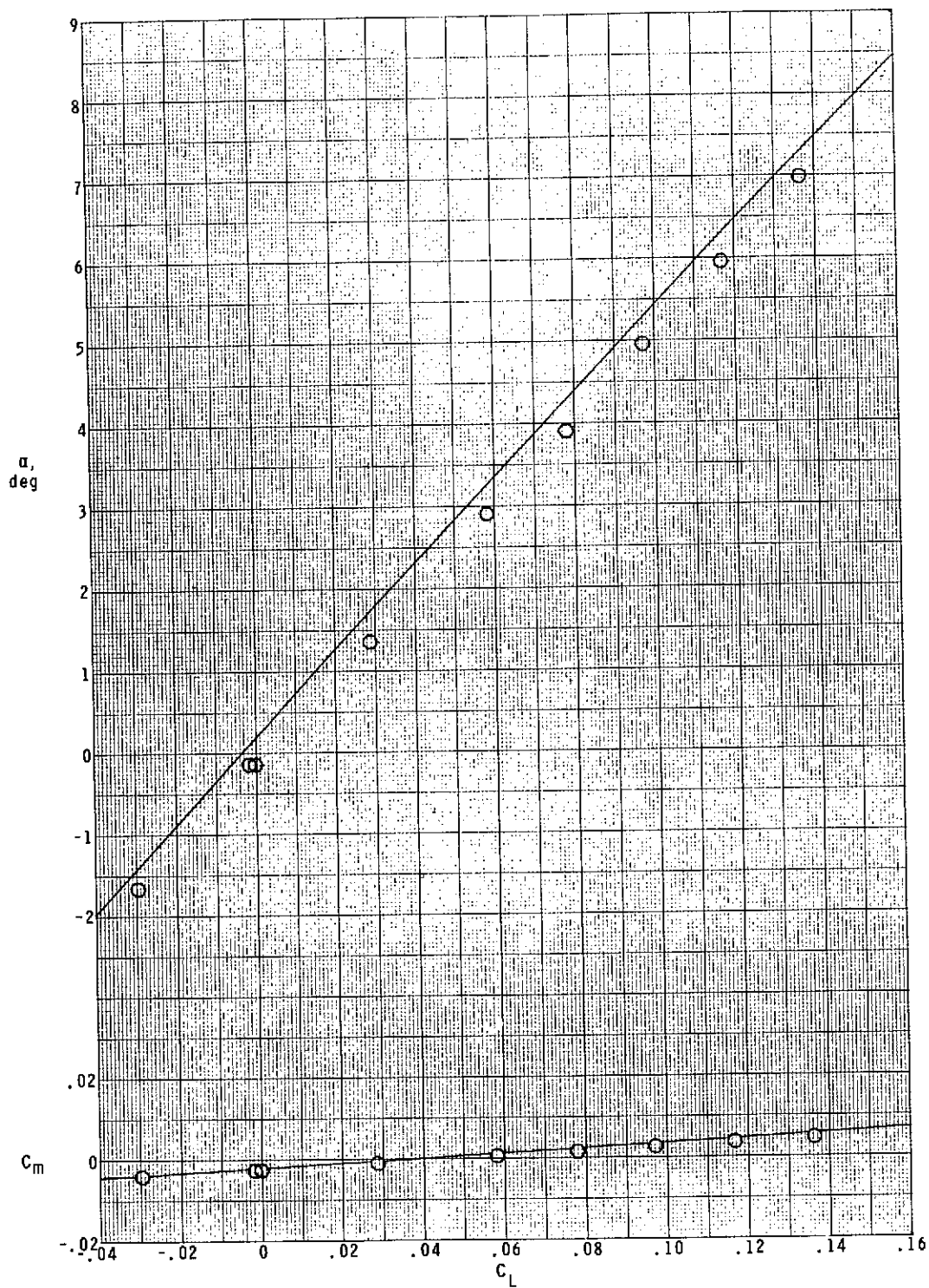
(b) $M = 4.63$.

Figure 9.- Continued.



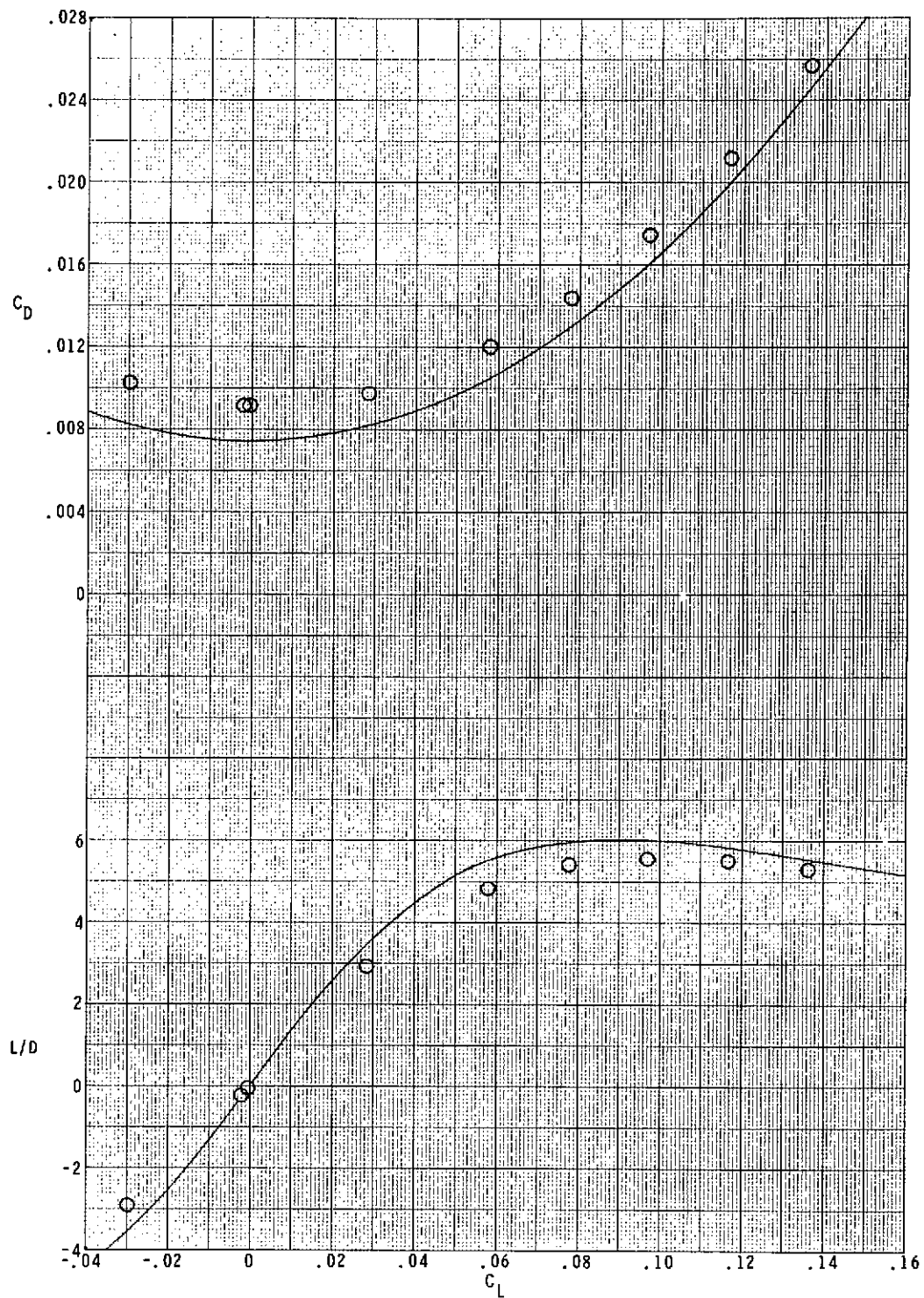
(b) $M = 4.63$. Concluded.

Figure 9.- Concluded.



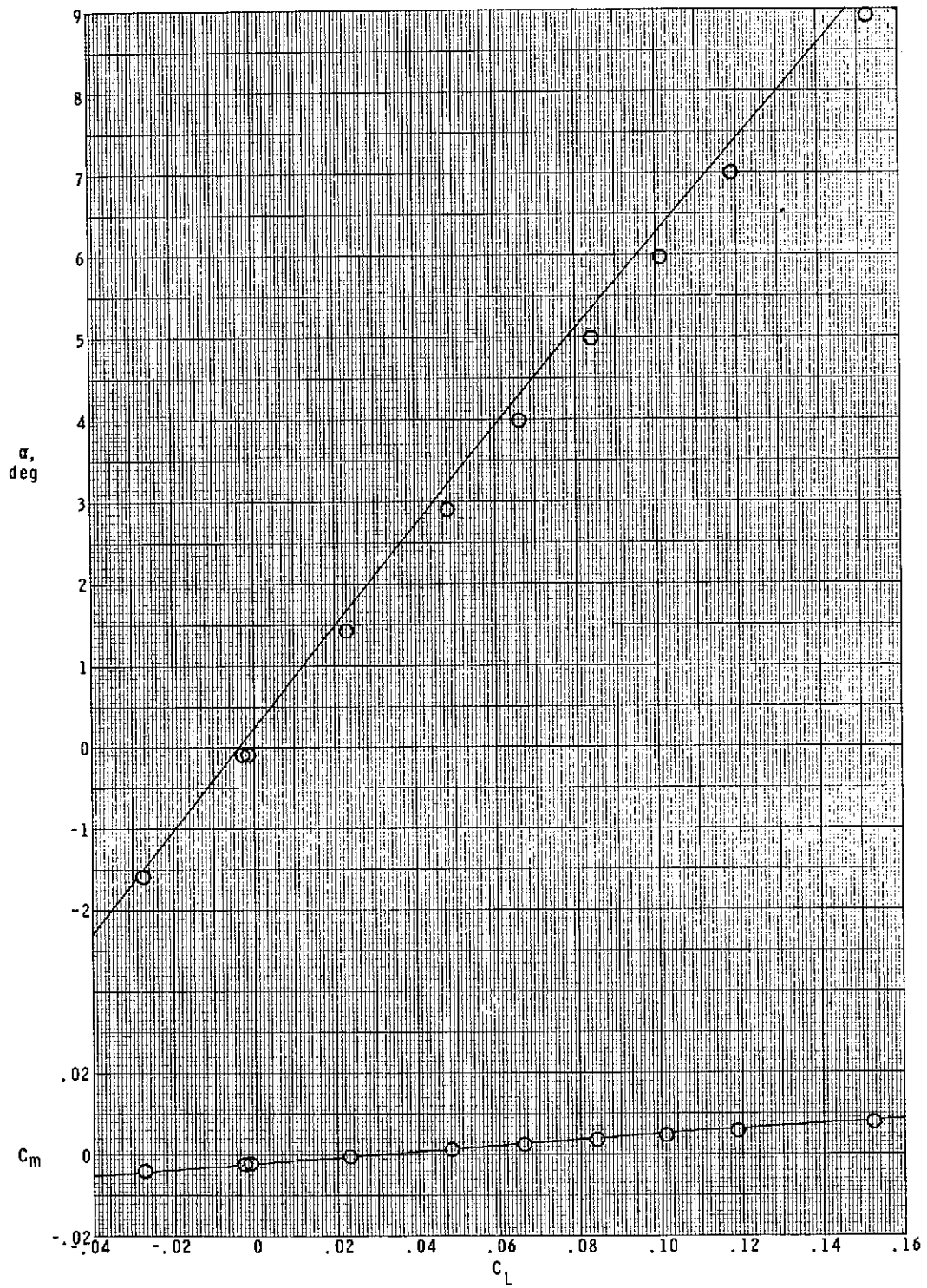
(a) $M = 3.95$.

Figure 10.- Comparison of wing 2 experimental data with two-dimensional shock-expansion predictions. Theory (solid line) includes viscous effects.



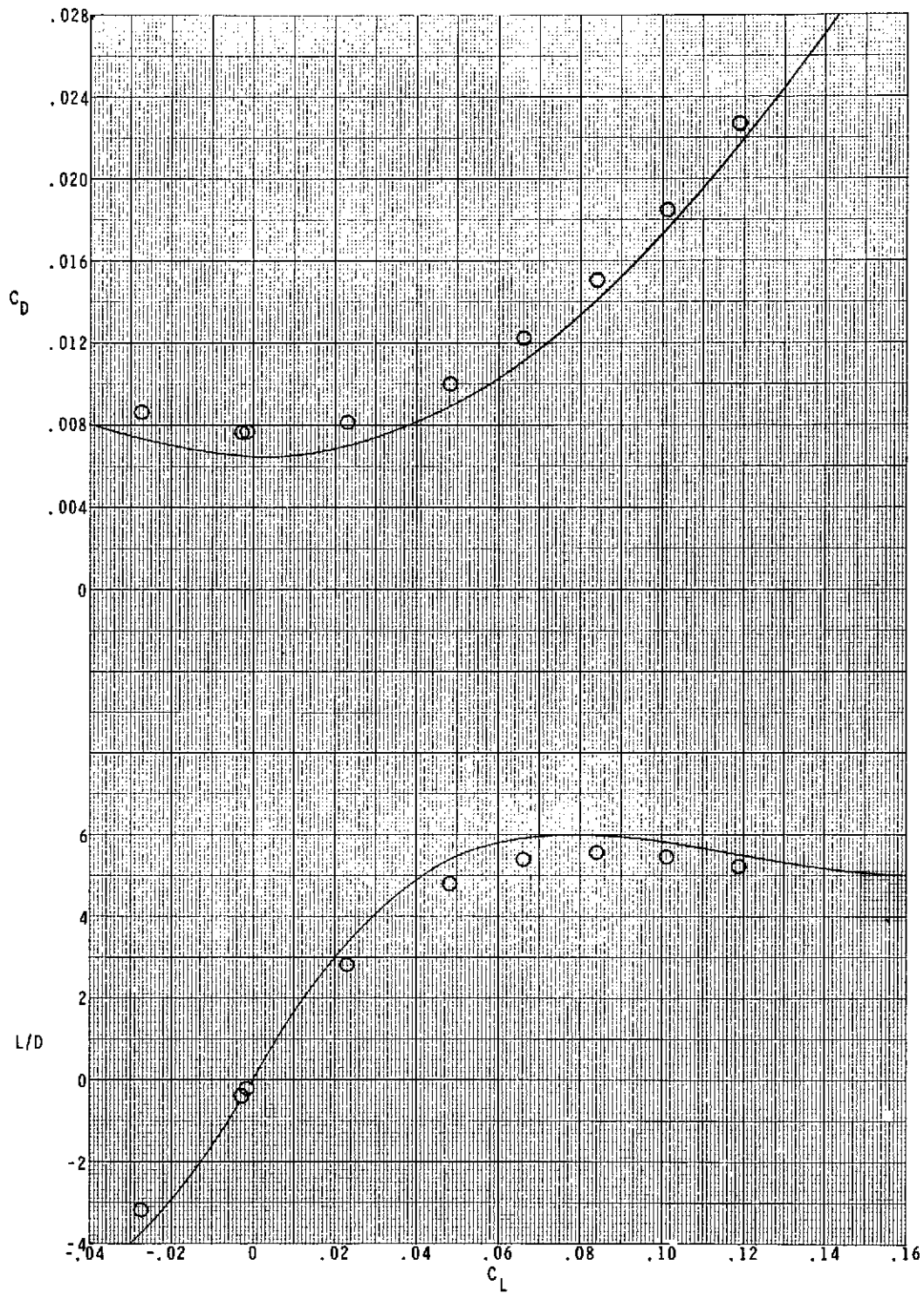
(a) $M = 3.95$. Concluded.

Figure 10.- Continued.



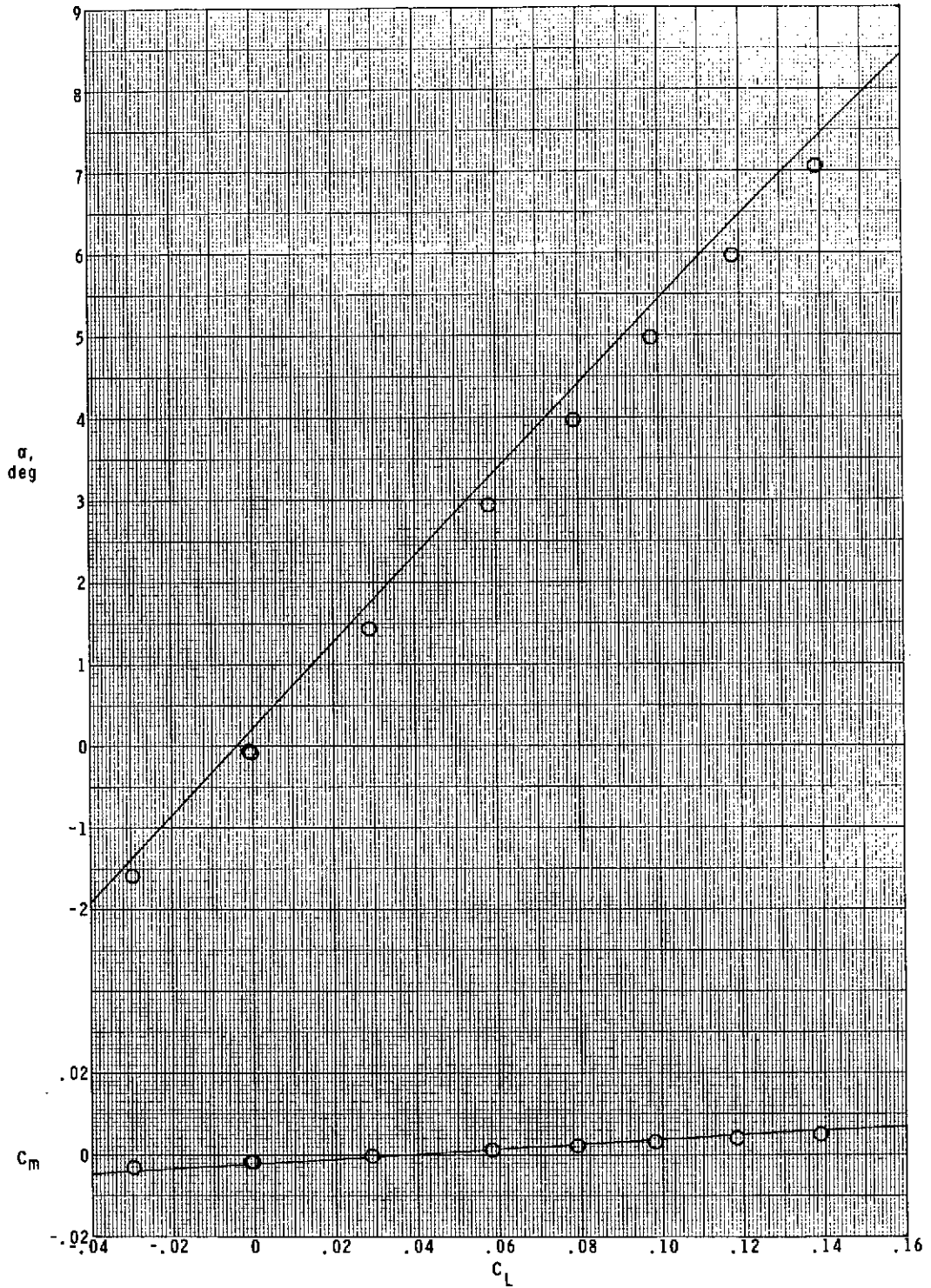
(b) $M = 4.63$.

Figure 10.- Continued.



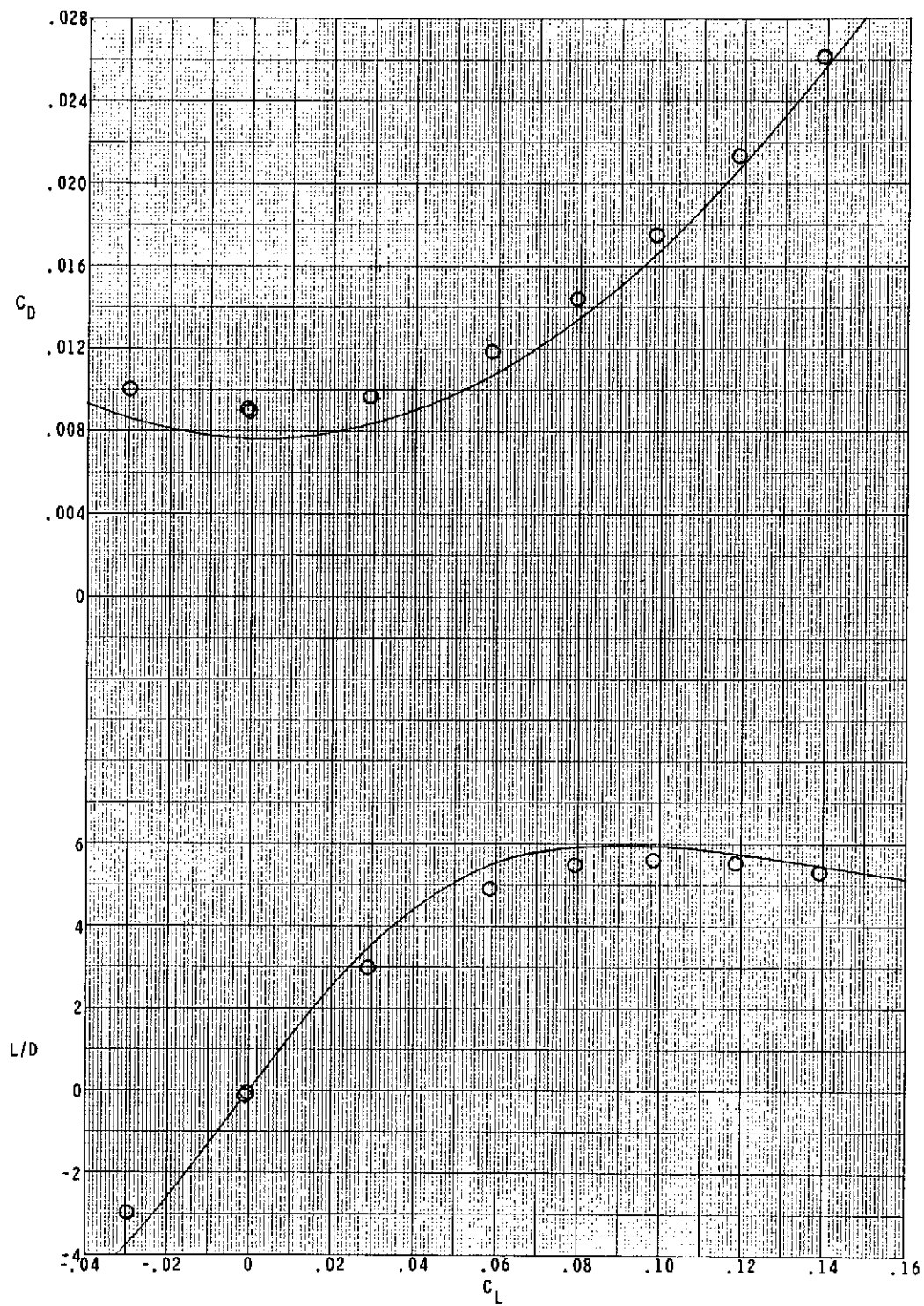
(b) $M = 4.63$. Concluded.

Figure 10.- Concluded.



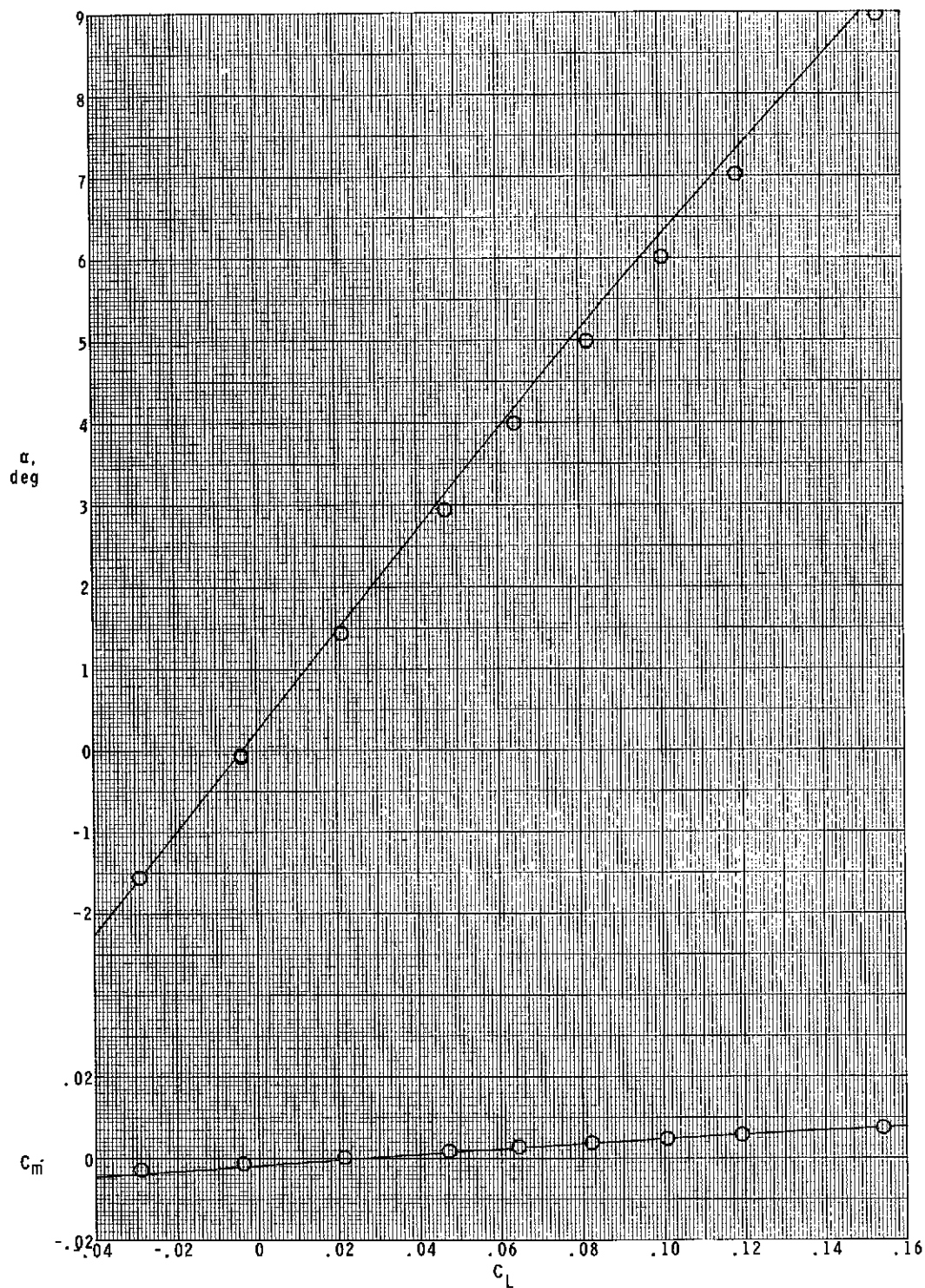
(a) $M = 3.95$.

Figure 11.- Comparison of wing 3 experimental data with two-dimensional shock-expansion predictions. Theory (solid line) includes viscous effects.



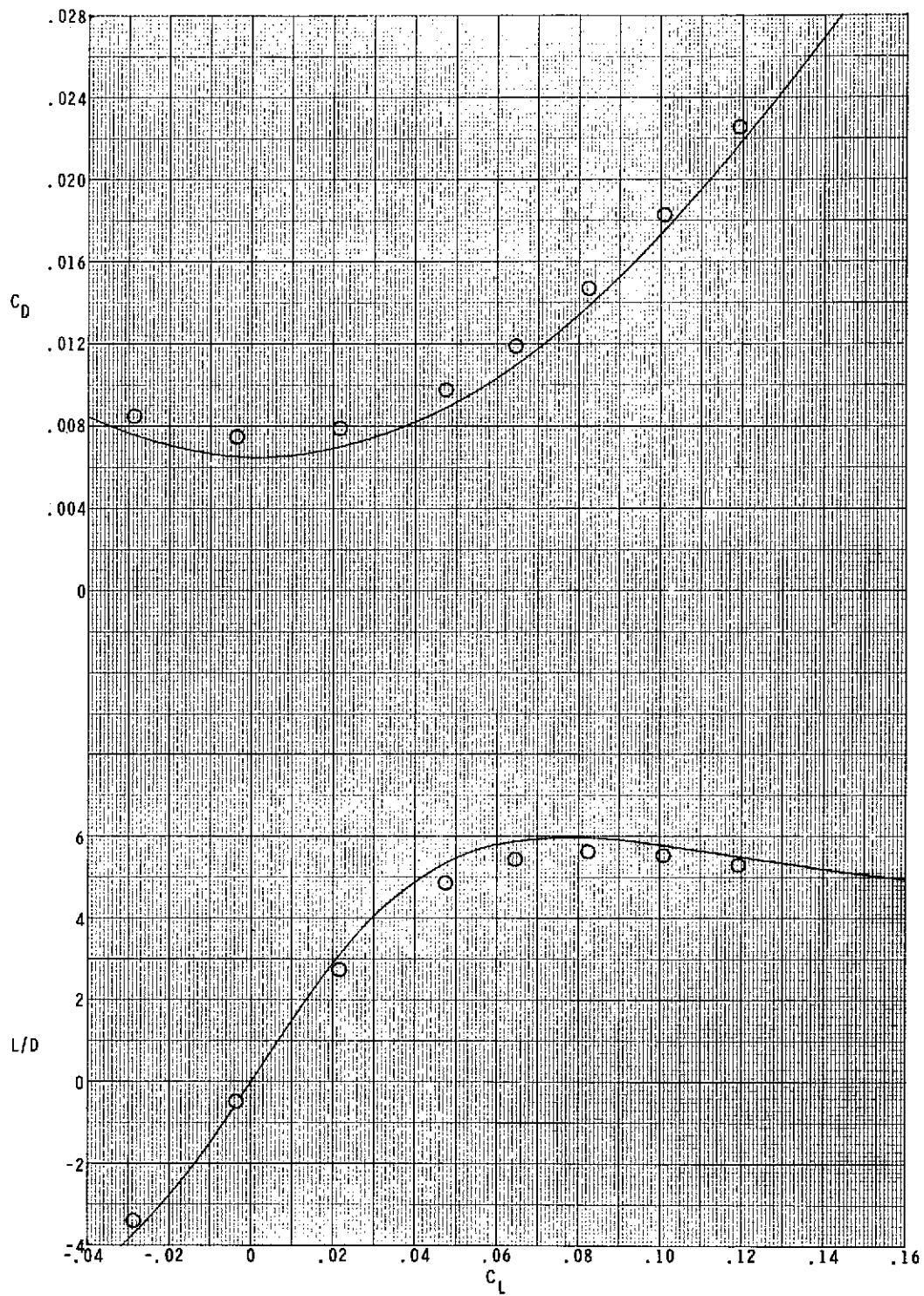
(a) $M = 3.95$. Concluded.

Figure 11.- Continued.



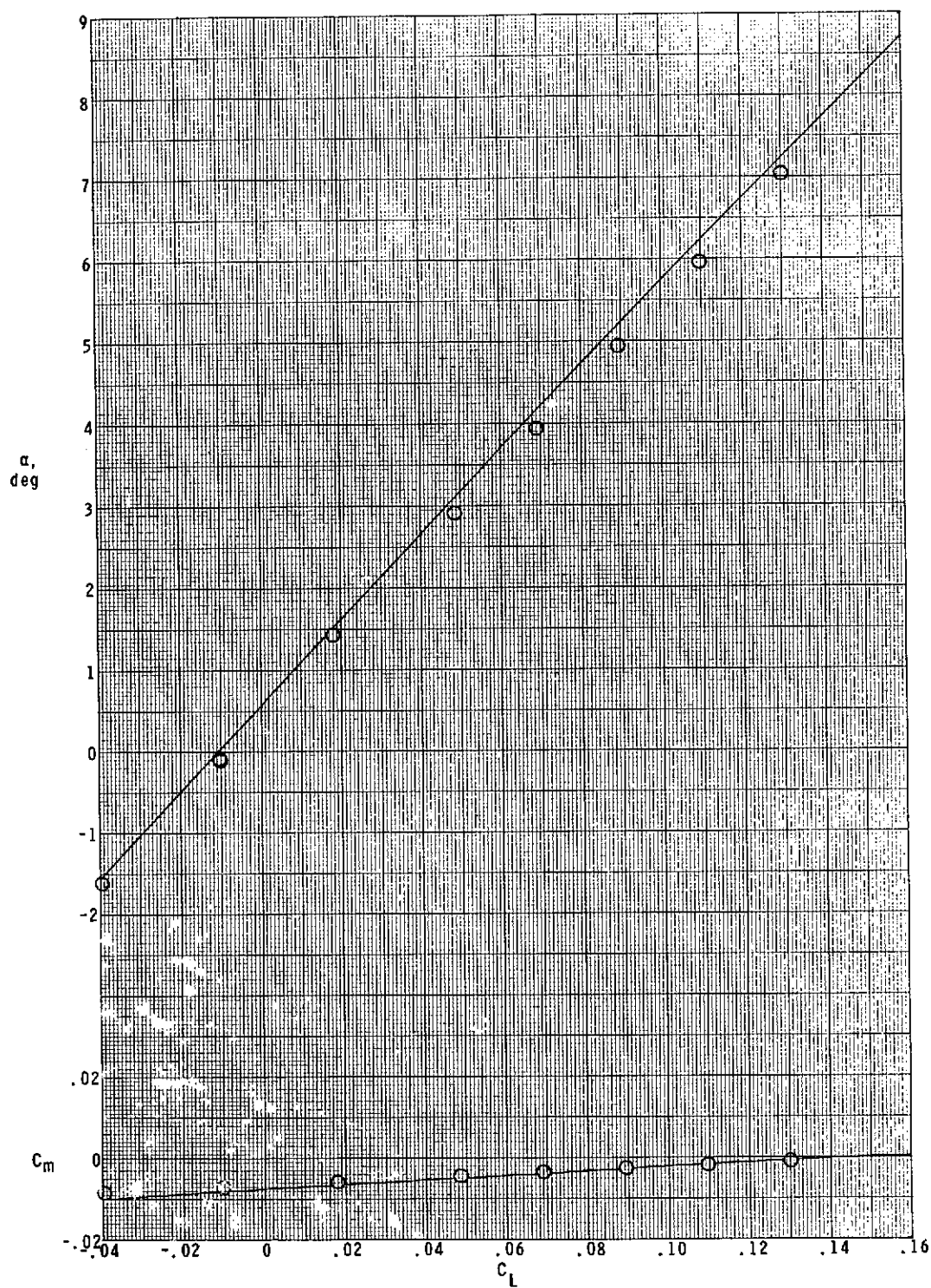
(b) $M = 4.63$.

Figure 11.- Continued.



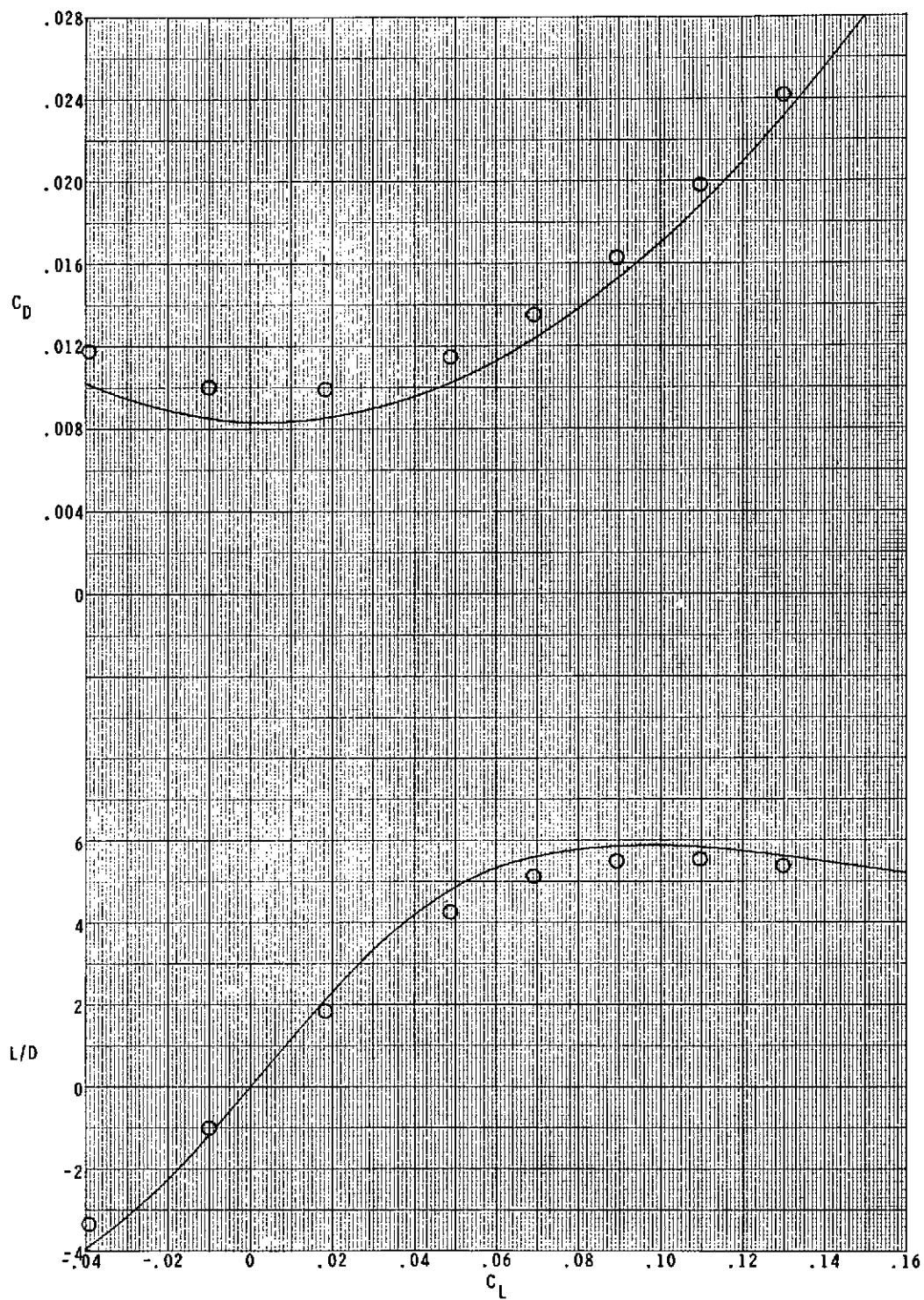
(b) $M = 4.63$. Concluded.

Figure 11. - Concluded.



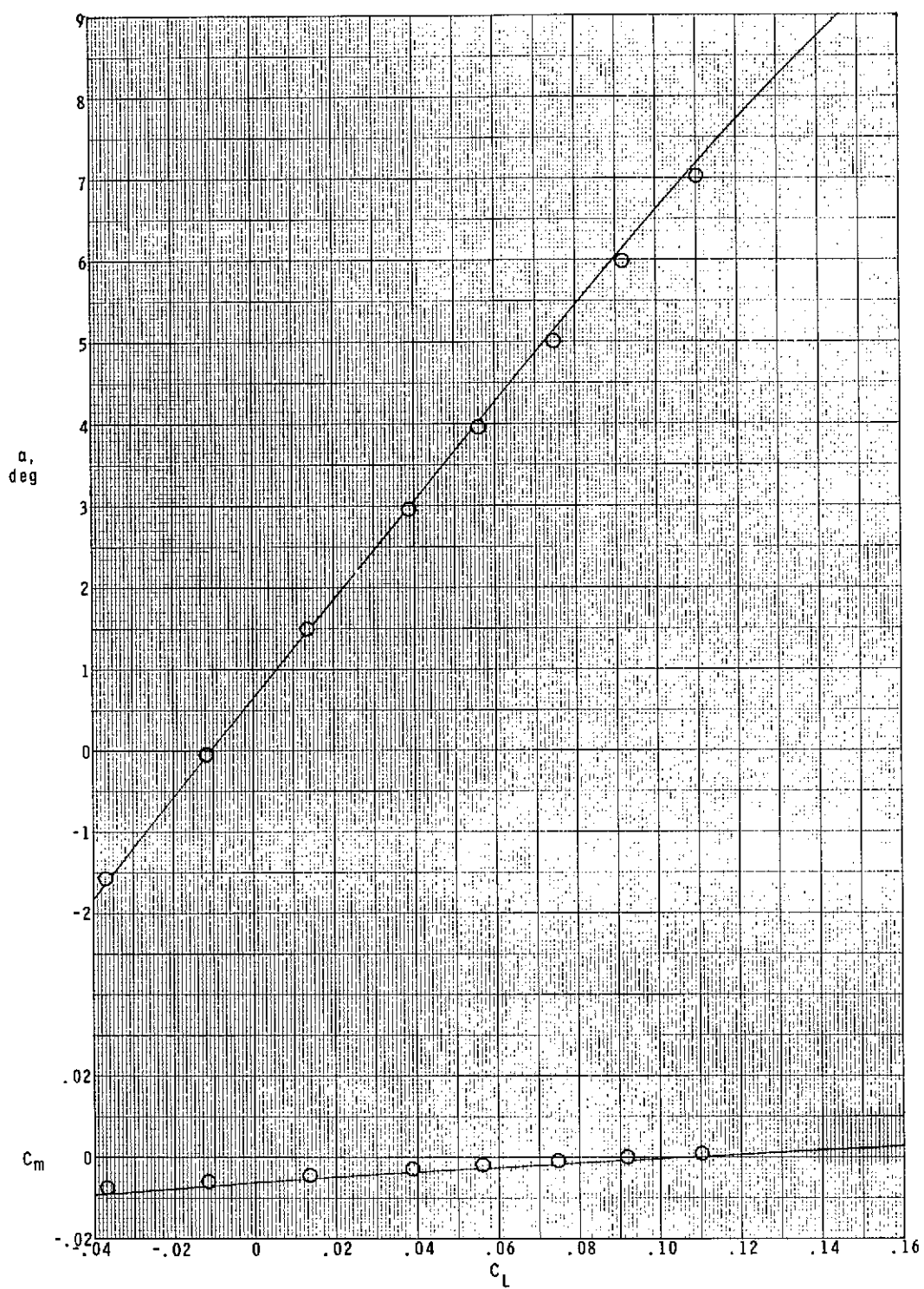
(a) $M = 3.95$.

Figure 12.- Comparison of wing 4 experimental data with two-dimensional shock-expansion predictions. Theory (solid line) includes viscous effects.



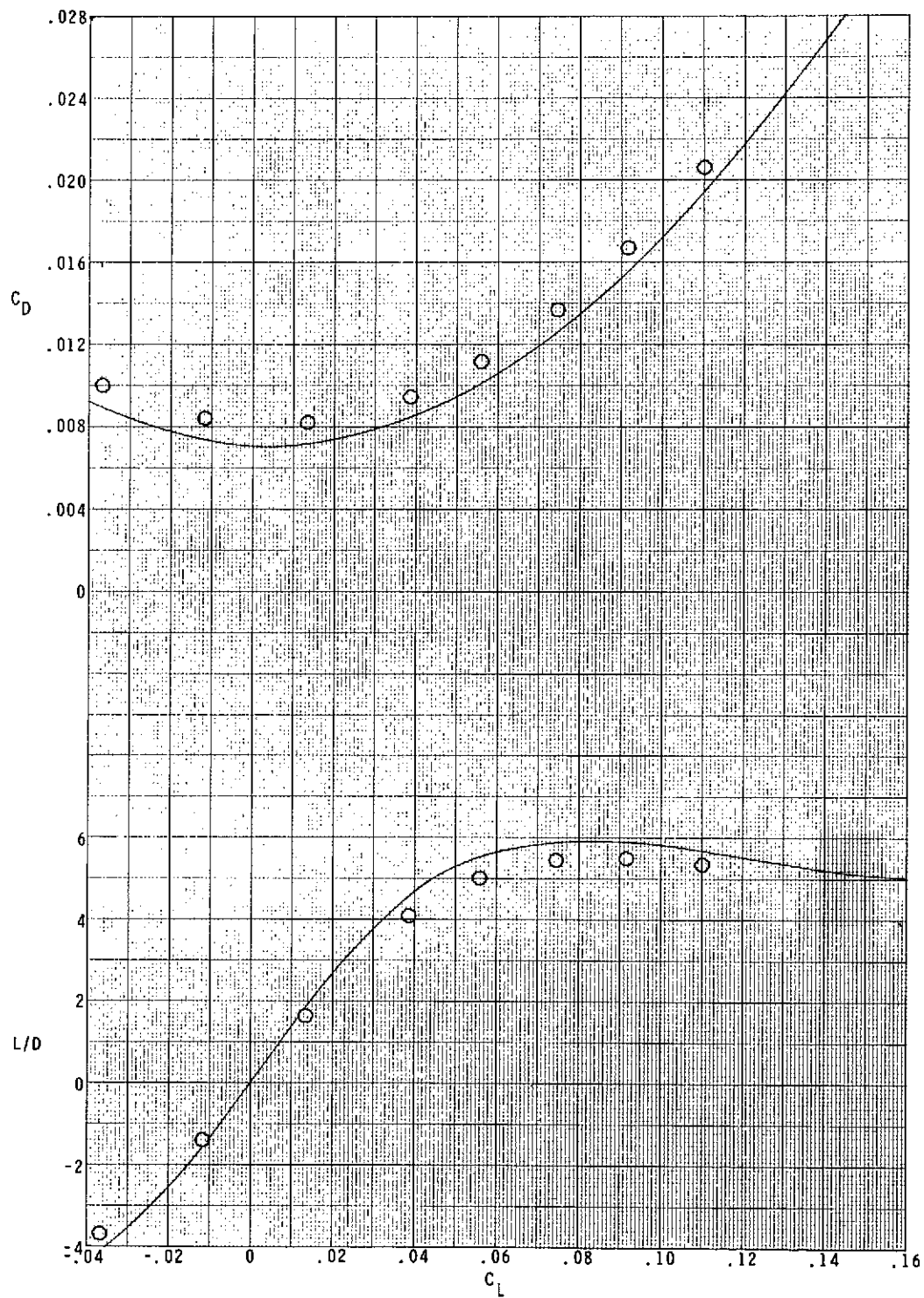
(a) $M = 3.95$. Concluded.

Figure 12.- Continued.



(b) $M = 4.63$.

Figure 12.- Continued.



(b) $M = 4.63$. Concluded.

Figure 12.- Concluded.

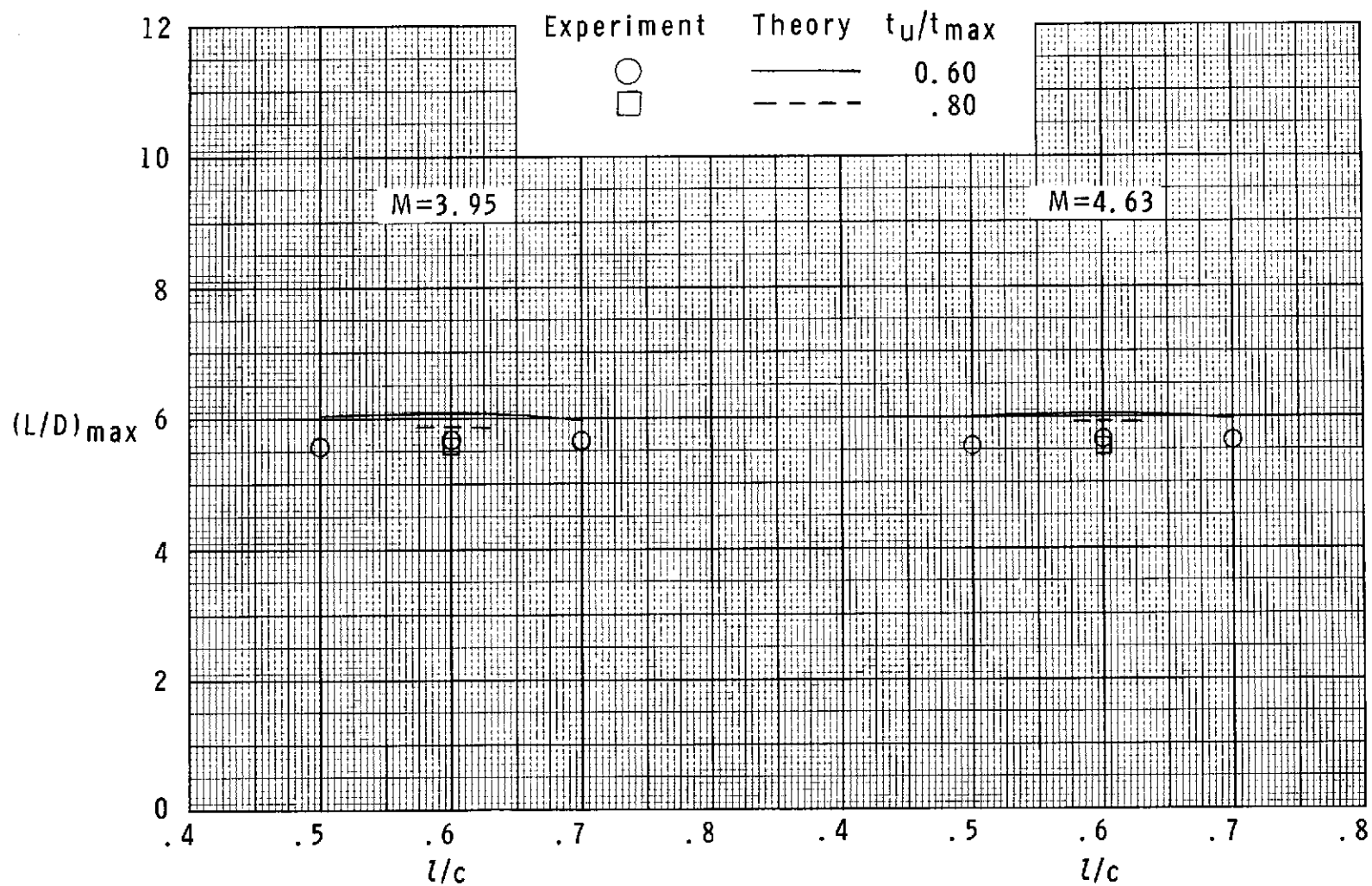


Figure 13.- Summary of experimental data and two-dimensional shock-expansion predictions.